28. Merkel, O.M.; Beyerle, A.; Librizzi, D.; Pfestroff, A.; Behr, T.M.; Sproat, B.; Barth, P.J.; Kissel, T. Nonviral siRNA delivery to the lung: investigation of PEG-PEI polyplexes and their *in vivo* performance. *Mol. Pharm.* **2009**, *6*, 1246–1260.
29. Garbuzenko, O.B.; Saad, M.; Betigeri, S.; Zhang, M.; Vetcher, A.A.; Soldatenkov, V.A.; Reimer, D.C.; Pozharov, V.P.; Minko, T. Intratracheal *versus* intravenous liposomal delivery of siRNA, antisense oligonucleotides and anticancer drug. *Pharm. Res.* **2009**, *26*, 382–394.
30. Wang, J.C.; Lai, S.; Guo, X.; Zhang, X.; de Crombrugghe, B.; Sonnylal, S.; Arnett, F.C.; Zhou, X. Attenuation of fibrosis *in vitro* and *in vivo* with SPARC siRNA. *Arthritis Res. Ther.* **2010**, doi: 10.1186/ar2973.
31. Gutbier, B.; Kube, S.M.; Reppe, K.; Santel, A.; Lange, C.; Kaufmann, J.; Suttorp, N.; Witzenrath, M. RNAi-mediated suppression of constitutive pulmonary gene expression by small interfering RNA in mice. *Pulm. Pharmacol. Ther.* **2010**, *23*, 334–344.
32. Driscoll, K.E.; Costa, D.L.; Hatch, G.; Henderson, R.; Oberdorster, G.; Salem, H.; Schlesinger, R.B. Intratracheal instillation as an exposure technique for the evaluation of respiratory tract toxicity: uses and limitations. *Toxicol. Sci.* **2000**, *55*, 24–35.
33. Bivas-Benita, M.; Zwier, R.; Junginger, H.E.; Borchard, G. Non-invasive pulmonary aerosol delivery in mice by the endotracheal route. *Eur. J. Pharm. Biopharm.* **2005**, *61*, 214–218.
34. Lu, D.; Hickey, A.J. Pulmonary vaccine delivery. *Expert Rev. Vaccines* **2007**, *6*, 213–226.
35. Bitko, V.; Musiyenko, A.; Shulyayeva, O.; Barik, S. Inhibition of respiratory viruses by nasally administered siRNA. *Nat. Med.* **2005**, *11*, 50–55.
36. Massaro, D.; Massaro, G.D.; Clerch, L.B. Noninvasive delivery of small inhibitory RNA and other reagents to pulmonary alveoli in mice. *Am. J. Physiol. Lung Cell Mol. Physiol.* **2004**, *287*, L1066–L1070.
37. Hickey, A.J.; Garcia-Contreras, L. Immunological and toxicological implications of short-term studies in animals of pharmaceutical aerosol delivery to the lungs: relevance to humans. *Crit. Rev. Ther. Drug Carrier. Syst.* **2001**, *18*, 387–431.
38. DeVincenzo, J.; Cehelsky, J.E.; Alvarez, R.; Elbashir, S.; Harborth, J.; Toudjarska, I.; Nechev, L.; Murugaiah, V.; Van Vliet, A.; Vaishnaw, A.K.; *et al.* Evaluation of the safety, tolerability and pharmacokinetics of ALN-RSV01, a novel RNAi antiviral therapeutic directed against respiratory syncytial virus (RSV). *Antiviral. Res.* **2008**, *77*, 225–231.
39. Mastrandrea, L.D.; Quattrin, T. Clinical evaluation of inhaled insulin. *Adv. Drug Deliv. Rev.* **2006**, *58*, 1061–1075.
40. Bai, S.; Gupta, V.; Ahsan, F. Inhalable lactose-based dry powder formulations of low molecular weight heparin. *J. Aerosol. Med. Pulm. Drug Deliv.* **2010**, *23*, 97–104.
41. Sanders, N.; Rudolph, C.; Braeckmans, K.; De Smedt, S.C.; Demeester, J. Extracellular barriers in respiratory gene therapy. *Adv. Drug Deliv. Rev.* **2009**, *61*, 115–127.
42. Roy, I.; Vij, N. Nanodelivery in airway diseases: Challenges and therapeutic applications. *Nanomedicine* **2010**, *6*, 237–244.
43. Groneberg, D.A.; Eynott, P.R.; Lim, S.; Oates, T.; Wu, R.; Carlstedt, I.; Roberts, P.; McCann, B.; Nicholson, A.G.; Harrison, B.D.; *et al.* Expression of respiratory mucins in fatal status asthmaticus and mild asthma. *Histopathology* **2002**, *40*, 367–373.

44. Jeffery, P.K. Remodeling in asthma and chronic obstructive lung disease. *Am. J. Respir. Crit. Care Med.* **2001**, *164*, S28–S38.
45. Lebhardt, T.; Roesler, S.; Beck-Broichsitter, M.; Kissel, T.; Polymeric nanocarriers for drug delivery to the lung. *J. Drug Deliv. Sci. Technol.* **2010**, *20*, 171–180.
46. Akhtar, S.; Benter, I.F. Nonviral delivery of synthetic siRNAs *in vivo*. *J. Clin. Invest.* **2007**, *117*, 3623–3632.
47. Goula, D.; Becker, N.; Lemkine, G.F.; Normandie, P.; Rodrigues, J.; Mantero, S.; Levi, G.; Demeneix, B.A. Rapid crossing of the pulmonary endothelial barrier by polyethylenimine/DNA complexes. *Gene Ther.* **2000**, *7*, 499–504.
48. Wang, J.; Lu, Z.; Wientjes, M.G.; Au, J.L. Delivery of siRNA therapeutics: Barriers and carriers. *AAPS J.* **2010**, *12*, 492–503.
49. Endoh, T.; Ohtsuki, T. Cellular siRNA delivery using cell-penetrating peptides modified for endosomal escape. *Adv. Drug Deliv. Rev.* **2009**, *61*, 704–709.
50. Novobrantseva, T.I.; Akinc, A.; Borodovsky, A.; de Fougerolles, A. Delivering silence: advancements in developing siRNA therapeutics. *Curr. Opin. Drug Discov. Devel.* **2008**, *11*, 217–224.
51. Shen, C.; Buck, A.K.; Liu, X.; Winkler, M.; Reske, S.N. Gene silencing by adenovirus-delivered siRNA. *FEBS Lett.* **2003**, *539*, 111–114.
52. Narvaiza, I.; Aparicio, O.; Vera, M.; Razquin, N.; Bortolanza, S.; Prieto, J.; Fortes, P. Effect of adenovirus-mediated RNA interference on endogenous microRNAs in a mouse model of multidrug resistance protein 2 gene silencing. *J. Virol.* **2006**, *80*, 12236–12247.
53. Guo, X.; Wang, W.; Hu, J.; Feng, K.; Pan, Y.; Zhang, L.; Feng, Y. Lentivirus-mediated RNAi knockdown of NUPR1 inhibits human nonsmall cell lung cancer growth *in vitro* and *in vivo*. *Anat. Rec.* **2012**, *295*, 2114–2121.
54. Scanlon, K.J. Cancer gene therapy: Challenges and opportunities. *Anticancer Res.* **2004**, *24*, 501–504.
55. Teichler Zallen, D. US gene therapy in crisis. *Trends Genet.* **2000**, *16*, 272–275.
56. Musiyenko, A.; Bitko, V.; Barik, S. RNAi-dependent and -independent antiviral phenotypes of chromosomally integrated shRNA clones: role of VASP in respiratory syncytial virus growth. *J. Mol. Med.* **2007**, *85*, 745–752.
57. Thomas, M.; Lu, J.J.; Chen, J.; Klibanov, A.M. Non-viral siRNA delivery to the lung. *Adv. Drug Deliv. Rev.* **2007**, *59*, 124–133.
58. Tseng, Y.C.; Mozumdar, S.; Huang, L. Lipid-based systemic delivery of siRNA. *Adv. Drug Deliv. Rev.* **2009**, *61*, 721–731.
59. Tompkins, S.M.; Lo, C.Y.; Tumpey, T.M.; Epstein, S.L. Protection against lethal influenza virus challenge by RNA interference *in vivo*. *Proc. Natl. Acad. Sci. USA* **2004**, *101*, 8682–8686.
60. Han, S.W.; Roman, J. Fibronectin induces cell proliferation and inhibits apoptosis in human bronchial epithelial cells: pro-oncogenic effects mediated by PI3-kinase and NF-kappa B. *Oncogene* **2006**, *25*, 4341–4349.
61. Thomas, M.; Lu, J.J.; Ge, Q.; Zhang, C.; Chen, J.; Klibanov, A.M. Full deacylation of polyethylenimine dramatically boosts its gene delivery efficiency and specificity to mouse lung. *Proc. Natl. Acad. Sci. USA* **2005**, *102*, 5679–5684.

62. Sioud, M.; Sorensen, D.R. Cationic liposome-mediated delivery of siRNAs in adult mice. *Biochem. Biophys. Res. Commun.* **2003**, *312*, 1220–1225.
63. Wu, S.Y.; McMillan, N.A. Lipidic systems for *in vivo* siRNA delivery. *AAPS J.* **2009**, *11*, 639–652.
64. Jackson, A.L.; Bartz, S.R.; Schelter, J.; Kobayashi, S.V.; Burchard, J.; Mao, M.; Li, B.; Cavet, G.; Linsley, P.S. Expression profiling reveals off-target gene regulation by RNAi. *Nat. Biotechnol.* **2003**, *21*, 635–637.
65. Bridge, A.J.; Pebernard, S.; Ducraux, A.; Nicoulaz, A.L.; Iggo, R. Induction of an interferon response by RNAi vectors in mammalian cells. *Nat. Genet.* **2003**, *34*, 263–264.
66. Heidel, J.D.; Hu, S.; Liu, X.F.; Triche, T.J.; Davis, M.E. Lack of interferon response in animals to naked siRNAs. *Nat. Biotechnol.* **2004**, *22*, 1579–1582.
67. Urban-Klein, B.; Werth, S.; Abuharbeid, S.; Czubayko, F.; Aigner, A. RNAi-mediated gene-targeting through systemic application of polyethylenimine (PEI)-complexed siRNA *in vivo*. *Gene Ther.* **2005**, *12*, 461–466.
68. Pal, A.; Ahmad, A.; Khan, S.; Sakabe, I.; Zhang, C.; Kasid, U.N.; Ahmad, I. Systemic delivery of RafsiRNA using cationic cardiolipin liposomes silences RAF-1 expression and inhibits tumor growth in xenograft model of human prostate cancer. *Int. J. Oncol.* **2005**, *26*, 1087–1091.
69. Nielsen, E.J.; Nielsen, J.M.; Becker, D.; Karlas, A.; Prakash, H.; Glud, S.Z.; Merrison, J.; Besenbacher, F.; Meyer, T.F.; Kjems, J.; Howard, K.A. Pulmonary gene silencing in transgenic EGFP mice using aerosolised chitosan/siRNA nanoparticles. *Pharm. Res.* **2010**, *27*, 2520–2527.
70. Akinc, A.; Zumbuehl, A.; Goldberg, M.; Leshchiner, E.S.; Busini, V.; Hossain, N.; Bacallado, S.A.; Nguyen, D.N.; Fuller, J.; Alvarez, R.; *et al.* A combinatorial library of lipid-like materials for delivery of RNAi therapeutics. *Nat. Biotechnol.* **2008**, *26*, 561–569.
71. Cosio, M.G.; Saetta, M.; Agusti, A. Immunologic aspects of chronic obstructive pulmonary disease. *New Engl. J. Med.* **2009**, *360*, 2445–2454.
72. Xu, L.; Anchordoquy, T. Drug delivery trends in clinical trials and translational medicine: challenges and opportunities in the delivery of nucleic acid-based therapeutics. *J. Pharm. Sci.* **2011**, *100*, 38–52.
73. Shen, J.; Samul, R.; Silva, R.L.; Akiyama, H.; Liu, H.; Saishin, Y.; Hackett, S.F.; Zinnen, S.; Kossen, K.; Fosnaugh, K.; *et al.* Suppression of ocular neovascularization with siRNA targeting VEGF receptor 1. *Gene Ther.* **2006**, *13*, 225–234.
74. The US National Institutes of Health. ClinicalTrials.gov. Available on line: http://www.clinicaltrials.gov/ (accessed on 30 November 2012).
75. Falsey, A.R.; Hennessey, P.A.; Formica, M.A.; Cox, C.; Walsh, E.E. Respiratory syncytial virus infection in elderly and high-risk adults. *New Engl. J. Med.* **2005**, *352*, 1749–1759.
76. Zamora, M.R.; Budev, M.; Rolfe, M.; Gottlieb, J.; Humar, A.; Devincenzo, J.; Vaishnaw, A.; Cehelsky, J.; Albert, G.; Nochur, S.; *et al.* RNA interference therapy in lung transplant patients infected with respiratory syncytial virus. *Am. J. Respir. Crit. Care Med.* **2011**, *183*, 531–538.
77. Dong, A.Q.; Kong, M.J.; Ma, Z.Y.; Qian, J.F.; Xu, X.H. Down-regulation of IGF-IR using small, interfering, hairpin RNA (siRNA) inhibits growth of human lung cancer cell line A549 *in vitro* and in nude mice. *Cell Biol. Int.* **2007**, *31*, 500–507.

78. Xia, H.; Yu, C.H.; Zhang, Y.; Yu, J.; Li, J.; Zhang, W.; Zhang, B.; Li, Y.; Guo, N. EZH2 silencing with RNAi enhances irradiation-induced inhibition of human lung cancer growth *in vitro* and *in vivo*. *Oncol. Lett.* **2012**, *4*, 135–140.
79. Aleku, M.; Schulz, P.; Keil, O.; Santel, A.; Schaeper, U.; Dieckhoff, B.; Janke, O.; Endruschat, J.; Durieux, B.; Roder, N.; *et al.* Atu027, a liposomal small interfering RNA formulation targeting protein kinase N3, inhibits cancer progression. *Cancer Res.* **2008**, *68*, 9788–9798.
80. Leenders, F.; Mopert, K.; Schmiedeknecht, A.; Santel, A.; Czauderna, F.; Aleku, M.; Penschuck, S.; Dames, S.; Sternberger, M.; Rohl, T.; *et al.* PKN3 is required for malignant prostate cell growth downstream of activated PI 3-kinase. *EMBO J.* **2004**, *23*, 3303–3313.
81. Katso, R.; Okkenhaug, K.; Ahmadi, K.; White, S.; Timms, J.; Waterfield, M.D. Cellular function of phosphoinositide 3-kinases: implications for development, homeostasis, and cancer. *Annu. Rev. Cell Dev. Biol.* **2001**, *17*, 615–675.
82. Hao, S.; Baltimore, D. The stability of mRNA influences the temporal order of the induction of genes encoding inflammatory molecules. *Nat. Immunol.* **2009**, *10*, 281–288.
83. Falk, J.A.; Minai, O.A.; Mosenifar, Z. Inhaled and systemic corticosteroids in chronic obstructive pulmonary disease. *Proc. Am. Thorac. Soc.* **2008**, *5*, 506–512.
84. Tsuji, T.; Aoshiba, K.; Nagai, A. Cigarette smoke induces senescence in alveolar epithelial cells. *Am. J. Respir. Cell Mol. Biol.* **2004**, *31*, 643–649.
85. Tuder, R.M.; Kern, J.A.; Miller, Y.E. Senescence in chronic obstructive pulmonary disease. *Proc. Am. Thorac. Soc.* **2012**, *9*, 62–63.
86. Molfino, N.A. Genetics of COPD. *Chest* **2004**, *125*, 1929–1940.
87. Chen, Z.H.; Kim, H.P.; Ryter, S.W.; Choi, A.M. Identifying targets for COPD treatment through gene expression analyses. *Int. J. Chron. Obstruct. Pulmon. Dis.* **2008**, *3*, 359–370.
88. Edwards, M.R.; Bartlett, N.W.; Clarke, D.; Birrell, M.; Belvisi, M.; Johnston, S.L. Targeting the NF-kappaB pathway in asthma and chronic obstructive pulmonary disease. *Pharmacol. Ther.* **2009**, *121*, 1–13.
89. Shapiro, S.D.; Goldstein, N.M.; Houghton, A.M.; Kobayashi, D.K.; Kelley, D.; Belaaouaj, A. Neutrophil elastase contributes to cigarette smoke-induced emphysema in mice. *Am. J. Pathol.* **2003**, *163*, 2329–2335.
90. Yoshida, T.; Tuder, R.M. Pathobiology of cigarette smoke-induced chronic obstructive pulmonary disease. *Physiol. Rev.* **2007**, *87*, 1047–1082.
91. Huang, S.L.; Su, C.H.; Chang, S.C. Tumor necrosis factor-alpha gene polymorphism in chronic bronchitis. *Am. J. Respir. Crit. Care Med.* **1997**, *156*, 1436–1439.
92. Stevenson, C.S.; Coote, K.; Webster, R.; Johnston, H.; Atherton, H.C.; Nicholls, A.; Giddings, J.; Sugar, R.; Jackson, A.; Press, N.J.; *et al.* Characterization of cigarette smoke-induced inflammatory and mucus hypersecretory changes in rat lung and the role of CXCR2 ligands in mediating this effect. *Am. J. Physiol. Lung Cell Mol. Physiol.* **2005**, *288*, 29.
93. Stevenson, C.S.; Docx, C.; Webster, R.; Battram, C.; Hynx, D.; Giddings, J.; Cooper, P.R.; Chakravarty, P.; Rahman, I.; Marwick, J.A.; *et al.* Comprehensive gene expression profiling of rat lung reveals distinct acute and chronic responses to cigarette smoke inhalation. *Am. J. Physiol. Lung Cell Mol. Physiol.* **2007**, *293*, L1183–L1193.

94. Aoshiba, K.; Yokohori, N.; Nagai, A. Alveolar wall apoptosis causes lung destruction and emphysematous changes. *Am. J. Respir. Cell Mol. Biol.* **2003**, *28*, 555–562.
95. Kasahara, Y.; Tuder, R.M.; Taraseviciene-Stewart, L.; Le Cras, T.D.; Abman, S.; Hirth, P.K.; Waltenberger, J.; Voelkel, N.F. Inhibition of VEGF receptors causes lung cell apoptosis and emphysema. *J. Clin. Invest.* **2000**, *106*, 1311–1319.
96. Barnes, P.J.; Stockley, R.A. COPD: current therapeutic interventions and future approaches. *Eur. Respir. J.* **2005**, *25*, 1084–1106.
97. Banerjee, A.; Koziol-White, C.; Panettieri, R., Jr. p38 MAPK inhibitors, IKK2 inhibitors, and TNFalpha inhibitors in COPD. *Curr. Opin. Pharmacol.* **2012**, *12*, 287–292.
98. World Health Organization. Chronic respiratory disease—Asthma. Available online: http://www.who.int/respiratory/asthma/en/ (accessed on 30 November 2012).
99. Huang, H.Y.; Chiang, B.L. siRNA as a therapy for asthma. *Curr. Opin. Mol. Ther.* **2009**, *11*, 652–663.
100. Meinicke, H.; Darcan, Y.; Hamelmann, E. Targeting allergic airway diseases by siRNA: An option for the future? *Curr. Mol. Med.* **2009**, *9*, 483–494.
101. Popescu, F.D. Antisense- and RNA interference-based therapeutic strategies in allergy. *J. Cell Mol. Med.* **2005**, *9*, 840–853.
102. Stenton, G.R.; Kim, M.K.; Nohara, O.; Chen, C.F.; Hirji, N.; Wills, F.L.; Gilchrist, M.; Hwang, P.H.; Park, J.G.; Finlay, W.; *et al.* Aerosolized Syk antisense suppresses Syk expression, mediator release from macrophages, and pulmonary inflammation. *J. Immunol.* **2000**, *164*, 3790–3797.
103. Ulanova, M.; Puttagunta, L.; Marcet-Palacios, M.; Duszyk, M.; Steinhoff, U.; Duta, F.; Kim, M.K.; Indik, Z.K.; Schreiber, A.D.; Befus, A.D. Syk tyrosine kinase participates in beta1-integrin signaling and inflammatory responses in airway epithelial cells. *Am. J. Physiol. Lung Cell Mol. Physiol.* **2005**, *288*, 19.
104. Winter, J.; Jung, S.; Keller, S.; Gregory, R.I.; Diederichs, S. Many roads to maturity: microRNA biogenesis pathways and their regulation. *Nat. Cell. Biol* **2009**, *11*, 228–234.
105. Pagdin, T.; Lavender, P. MicroRNAs in lung diseases. *Thorax* **2012**, *67*, 183–184.
106. Trang, P.; Medina, P.P.; Wiggins, J.F.; Ruffino, L.; Kelnar, K.; Omotola, M.; Homer, R.; Brown, D.; Bader, A.G.; Weidhaas, J.B.; *et al.* Regression of murine lung tumors by the let-7 microRNA. *Oncogene* **2010**, *29*, 1580–1587.
107. Wiggins, J.F.; Ruffino, L.; Kelnar, K.; Omotola, M.; Patrawala, L.; Brown, D.; Bader, A.G. Development of a lung cancer therapeutic based on the tumor suppressor microRNA-34. *Cancer Res.* **2010**, *70*, 5923–5930.
108. Liu, C.; Kelnar, K.; Liu, B.; Chen, X.; Calhoun-Davis, T.; Li, H.; Patrawala, L.; Yan, H.; Jeter, C.; Honorio, S.; *et al.* The microRNA miR-34a inhibits prostate cancer stem cells and metastasis by directly repressing CD44. *Nat. Med.* **2011**, *17*, 211–215.
109. Van Rooij, E.; Sutherland, L.B.; Thatcher, J.E.; DiMaio, J.M.; Naseem, R.H.; Marshall, W.S.; Hill, J.A.; Olson, E.N. Dysregulation of microRNAs after myocardial infarction reveals a role of miR-29 in cardiac fibrosis. *Proc. Natl. Acad. Sci. USA* **2008**, *105*, 13027–13032.
110. Lanford, R.E.; Hildebrandt-Eriksen, E.S.; Petri, A.; Persson, R.; Lindow, M.; Munk, M.E.; Kauppinen, S.; Orum, H. Therapeutic silencing of microRNA-122 in primates with chronic hepatitis C virus infection. *Science* **2010**, *327*, 198–201.

111. van Rooij, E.; Sutherland, L.B.; Qi, X.; Richardson, J.A.; Hill, J.; Olson, E.N. Control of stress-dependent cardiac growth and gene expression by a microRNA. *Science* **2007**, *316*, 575–579.
112. Porrello, E.R.; Johnson, B.A.; Aurora, A.B.; Simpson, E.; Nam, Y.J.; Matkovich, S.J.; Dorn, G.W., II.; van Rooij, E.; Olson, E.N. MiR-15 family regulates postnatal mitotic arrest of cardiomyocytes. *Circ. Res.* **2011**, *109*, 670–679.
113. Zhu, H.; Yang, Y.; Wang, Y.; Li, J.; Schiller, P.W.; Peng, T. MicroRNA-195 promotes palmitate-induced apoptosis in cardiomyocytes by down-regulating Sirt1. *Cardiovasc. Res.* **2011**, *92*, 75–84.
114. Williams, A.H.; Valdez, G.; Moresi, V.; Qi, X.; McAnally, J.; Elliott, J.L.; Bassel-Duby, R.; Sanes, J.R.; Olson, E.N. MicroRNA-206 delays ALS progression and promotes regeneration of neuromuscular synapses in mice. *Science* **2009**, *326*, 1549–1554.
115. Patrick, D.M.; Zhang, C.C.; Tao, Y.; Yao, H.; Qi, X.; Schwartz, R.J.; Jun-Shen Huang, L.; Olson, E.N. Defective erythroid differentiation in miR-451 mutant mice mediated by 14–3-3zeta. *Genes Dev.* **2010**, *24*, 1614–1619.
116. Lewis, A.; Riddoch-Contreras, J.; Natanek, S.A.; Donaldson, A.; Man, W.D.; Moxham, J.; Hopkinson, N.S.; Polkey, M.I.; Kemp, P.R. Downregulation of the serum response factor/miR-1 axis in the quadriceps of patients with COPD. *Thorax* **2012**, *67*, 26–34.
117. Pottelberge, G.R.; Mestdagh, P.; Bracke, K.R.; Thas, O.; Durme, Y.M.; Joos, G.F.; Vandesompele, J.; Brusselle, G.G. MicroRNA expression in induced sputum of smokers and patients with chronic obstructive pulmonary disease. *Am. J. Respir. Crit. Care Med.* **2011**, *183*, 898–906.
118. Liu, G.; Friggeri, A.; Yang, Y.; Milosevic, J.; Ding, Q.; Thannickal, V.J.; Kaminski, N.; Abraham, E. miR-21 mediates fibrogenic activation of pulmonary fibroblasts and lung fibrosis. *J. Exp. Med.* **2010**, *207*, 1589–1597.
119. Pandit, K.V.; Corcoran, D.; Yousef, H.; Yarlagadda, M.; Tzouvelekis, A.; Gibson, K.F.; Konishi, K.; Yousem, S.A.; Singh, M.; Handley, D.; *et al.* Inhibition and role of let-7d in idiopathic pulmonary fibrosis. *Am. J. Respir. Crit. Care Med.* **2010**, *182*, 220–229.
120. Cushing, L.; Kuang, P.P.; Qian, J.; Shao, F.; Wu, J.; Little, F.; Thannickal, V.J.; Cardoso, W.V.; Lu, J. miR-29 is a major regulator of genes associated with pulmonary fibrosis. *Am. J. Respir. Cell Mol. Biol.* **2011**, *45*, 287–294.
121. Yang, S.; Banerjee, S.; de Freitas, A.; Sanders, Y.Y.; Ding, Q.; Matalon, S.; Thannickal, V.J.; Abraham, E.; Liu, G. Participation of miR-200 in pulmonary fibrosis. *Am. J. Pathol.* **2012**, *180*, 484–493.
122. Rodriguez, A.; Vigorito, E.; Clare, S.; Warren, M.V.; Couttet, P.; Soond, D.R.; van Dongen, S.; Grocock, R.J.; Das, P.P.; Miska, E.A.; *et al.* Requirement of bic/microRNA-155 for normal immune function. *Science* **2007**, *316*, 608–611.
123. Lu, T.X.; Munitz, A.; Rothenberg, M.E. MicroRNA-21 is up-regulated in allergic airway inflammation and regulates IL-12p35 expression. *J. Immunol.* **2009**, *182*, 4994–5002.
124. Mattes, J.; Collison, A.; Plank, M.; Phipps, S.; Foster, P.S. Antagonism of microRNA-126 suppresses the effector function of TH2 cells and the development of allergic airways disease. *Proc. Natl. Acad. Sci. USA* **2009**, *106*, 18704–18709.

125. Chiba, Y.; Tanabe, M.; Goto, K.; Sakai, H.; Misawa, M. Down-regulation of miR-133a contributes to up-regulation of Rhoa in bronchial smooth muscle cells. *Am. J. Respir. Crit. Care Med.* **2009**, *180*, 713–719.
126. Ezzie, M.E.; Crawford, M.; Cho, J.H.; Orellana, R.; Zhang, S.; Gelinas, R.; Batte, K.; Yu, L.; Nuovo, G.; Galas, D.; *et al.* Gene expression networks in COPD: microRNA and mRNA regulation. *Thorax* **2012**, *67*, 122–131.
127. Sato, T.; Liu, X.; Nelson, A.; Nakanishi, M.; Kanaji, N.; Wang, X.; Kim, M.; Li, Y.; Sun, J.; Michalski, J.; *et al.* Reduced miR-146a increases prostaglandin E(2)in chronic obstructive pulmonary disease fibroblasts. *Am. J. Respir. Crit. Care Med.* **2010**, *182*, 1020–1029.
128. Pottier, N.; Maurin, T.; Chevalier, B.; Puissegur, M.P.; Lebrigand, K.; Robbe-Sermesant, K.; Bertero, T.; Lino Cardenas, C.L.; Courcot, E.; Rios, G.; *et al.* Identification of keratinocyte growth factor as a target of microRNA-155 in lung fibroblasts: Implication in epithelial-mesenchymal interactions. *PLoS One* **2009**, doi:10.1371/journal.pone.0006718.
129. Izzotti, A.; Calin, G.A.; Arrigo, P.; Steele, V.E.; Croce, C.M.; de Flora, S. Downregulation of microRNA expression in the lungs of rats exposed to cigarette smoke. *FASEB J.* **2009**, *23*, 806–812.
130. Schembri, F.; Sridhar, S.; Perdomo, C.; Gustafson, A.M.; Zhang, X.; Ergun, A.; Lu, J.; Liu, G.; Zhang, X.; Bowers, J.; *et al.* MicroRNAs as modulators of smoking-induced gene expression changes in human airway epithelium. *Proc. Natl. Acad. Sci. USA* **2009**, *106*, 2319–2324.
131. Decramer, M.; Rennard, S.; Troosters, T.; Mapel, D.W.; Giardino, N.; Mannino, D.; Wouters, E.; Sethi, S.; Cooper, C.B. COPD as a lung disease with systemic consequences--clinical impact, mechanisms, and potential for early intervention. *COPD* **2008**, *5*, 235–256.
132. Gower, A.C.; Steiling, K.; Brothers, J.F., II.; Lenburg, M.E.; Spira, A. Transcriptomic studies of the airway field of injury associated with smoking-related lung disease. *Proc. Am. Thorac. Soc.* **2011**, *8*, 173–179.
133. Agusti, A.G. COPD, a multicomponent disease: implications for management. *Respir. Med.* **2005**, *99*, 670–682.
134. Locksley, R.M. Asthma and allergic inflammation. *Cell* **2010**, *140*, 777–783.
135. Williams, A.E.; Larner-Svensson, H.; Perry, M.M.; Campbell, G.A.; Herrick, S.E.; Adcock, I.M.; Erjefalt, J.S.; Chung, K.F.; Lindsay, M.A. MicroRNA expression profiling in mild asthmatic human airways and effect of corticosteroid therapy. *PLoS One* **2009**, doi:10.1371/journal.pone.0005889.
136. Oglesby, I.K.; McElvaney, N.G.; Greene, C.M. MicroRNAs in inflammatory lung disease--master regulators or target practice? *Respir. Res.* **2010**, *11*, 148.
137. Boudreau, R.L.; Martins, I.; Davidson, B.L. Artificial microRNAs as siRNA shuttles: improved safety as compared to shRNAs *in vitro* and *in vivo*. *Mol. Ther.* **2009**, *17*, 169–175.
138. Bader, A.G.; Brown, D.; Winkler, M. The promise of microRNA replacement therapy. *Cancer Res.* **2010**, *70*, 7027–7030.
139. Johnson, S.M.; Grosshans, H.; Shingara, J.; Byrom, M.; Jarvis, R.; Cheng, A.; Labourier, E.; Reinert, K.L.; Brown, D.; Slack, F.J. RAS is regulated by the let-7 microRNA family. *Cell* **2005**, *120*, 635–647.

140. He, X.Y.; Chen, J.X.; Zhang, Z.; Li, C.L.; Peng, Q.L.; Peng, H.M. The let-7a microRNA protects from growth of lung carcinoma by suppression of k-Ras and c-Myc in nude mice. *J. Cancer Res. Clin. Oncol.* **2010**, *136*, 1023–1028.
141. Esquela-Kerscher, A.; Trang, P.; Wiggins, J.F.; Patrawala, L.; Cheng, A.; Ford, L.; Weidhaas, J.B.; Brown, D.; Bader, A.G.; Slack, F.J. The let-7 microRNA reduces tumor growth in mouse models of lung cancer. *Cell Cycle* **2008**, *7*, 759–764.
142. Chen, Y.; Zhu, X.; Zhang, X.; Liu, B.; Huang, L. Nanoparticles modified with tumor-targeting scFv deliver siRNA and miRNA for cancer therapy. *Mol. Ther.* **2010**, *18*, 1650–1656.
143. Ling, B.; Wang, G.X.; Long, G.; Qiu, J.H.; Hu, Z.L. Tumor suppressor miR-22 suppresses lung cancer cell progression through post-transcriptional regulation of ErbB3. *J. Cancer Res. Clin. Oncol.* **2012**, *138*, 1355–1361.
144. Krutzfeldt, J.; Rajewsky, N.; Braich, R.; Rajeev, K.G.; Tuschl, T.; Manoharan, M.; Stoffel, M. Silencing of microRNAs *in vivo* with "antagomirs". *Nature* **2005**, *438*, 685–689.
145. Elmen, J.; Lindow, M.; Schutz, S.; Lawrence, M.; Petri, A.; Obad, S.; Lindholm, M.; Hedtjarn, M.; Hansen, H.F.; Berger, U.; *et al.* LNA-mediated microRNA silencing in non-human primates. *Nature* **2008**, *452*, 896–899.
146. Li, Y.J.; Zhang, Y.X.; Wang, P.Y.; Chi, Y.L.; Zhang, C.; Ma, Y.; Lv, C.J.; Xie, S.Y. Regression of A549 lung cancer tumors by anti-miR-150 vector. *Oncol. Rep.* **2012**, *27*, 129–134.
147. Zheng, T.; Wang, J.; Chen, X.; Liu, L. Role of microRNA in anticancer drug resistance. *Int. J. Cancer* **2010**, *126*, 2–10.
148. Ji, Q.; Hao, X.; Zhang, M.; Tang, W.; Yang, M.; Li, L.; Xiang, D.; Desano, J.T.; Bommer, G.T.; Fan, D.; *et al.* MicroRNA miR-34 inhibits human pancreatic cancer tumor-initiating cells. *PLoS One* **2009**, *4*, doi:10.1371/journal.pone.0006816.

SCIENTIFIC REPORTS

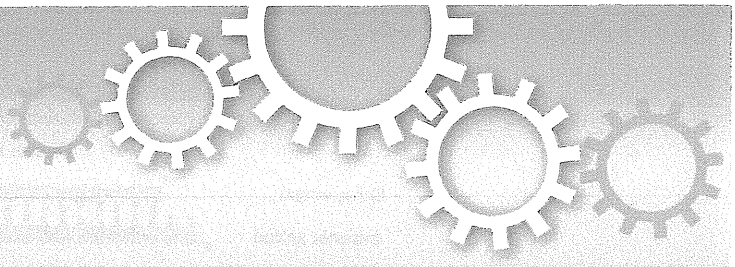

OPEN

SUBJECT AREAS:
DRUG DEVELOPMENT
DRUG DELIVERY
RNAI
LUNG CANCER

Received
22 April 2013

Accepted
8 November 2013

Published
25 November 2013

Correspondence and requests for materials should be addressed to T.O. (tochiya@ncc.go.jp)

A novel platform to enable inhaled naked RNAi medicine for lung cancer

Yu Fujita[1,2], Fumitaka Takeshita[1], Takayuki Mizutani[3], Tadaaki Ohgi[3], Kazuyoshi Kuwano[2] & Takahiro Ochiya[1]

[1]Division of Molecular and Cellular Medicine, National Cancer Center Research Institute, 5-1-1, Tsukiji, Chuo-ku, Tokyo 104-0045, Japan, [2]Division of Respiratory Diseases, Department of Internal Medicine, Jikei University School of Medicine, 3-19-18, Nishi-shinbashi, Minato-ku, Tokyo 105-8471, Japan, [3]BONAC Corporation, Fukuoka BIO Factory 4F, 1488-4, Aikawa-machi, Kurume-shi, Fukuoka 839-0861, Japan.

Small interfering RNA (siRNA)-based therapeutics have been used in humans and offer distinct advantages over traditional therapies. However, previous investigations have shown that there are several technical obstacles that need to be overcome before routine clinical applications are used. Currently, we are launching a novel class of RNAi therapeutic agents (PnkRNA™, nkRNA®) that show high resistance to degradation and are less immunogenic, less cytotoxic, and capable of efficient intracellular delivery. Here, we develop a novel platform to promote naked RNAi approaches administered through inhalation without sophisticated delivery technology in mice. Furthermore, a naked and unmodified novel RNAi agent, such as ribophorin II (RPN2-PnkRNA), which has been selected as a therapeutic target for lung cancer, resulted in efficient inhibition of tumor growth without any significant toxicity. Thus, this new technology using aerosol delivery could represent a safe, potentially RNAi-based strategy for clinical applications in lung cancer treatment without delivery vehicles.

RNA interference (RNAi) is a post-transcriptional gene-silencing mechanism. Small interfering RNA (siRNA) must be dissociated into their component single strands to act as a guide for the RNA-induced silencing complexes, which are the protein complexes that repress gene expression[1]. The development of siRNA technology has opened an avenue of opportunity to study gene function, as well as the possibility of novel forms of therapeutic intervention in several genetic diseases. In fact, siRNA-based therapy has enormous potential for the treatment of several diseases through either local or systemic administration of siRNAs that are being tested in experimental animal models or in clinical development[2]. Oncology is one of the medical fields that can benefit most from this powerful therapeutic strategy because this approach can modulate the expression of target genes involved in tumor initiation, growth, and metastasis[3].

However, the clinical application of siRNAs has been impaired by problems related to their delivery, low biological stability, off-target gene silencing, and immunostimulatory effects[4,5]. Indeed, naked siRNAs are promptly degraded by nucleases in serum and extracellular fluids, and chemical modifications at specific positions or formulations with delivery vehicles have been shown to improve stability. However, these may attenuate the suppressive activity of siRNAs[6]. Furthermore, the cost of large-scale production is another obstacle to the clinical application of siRNAs[7]. For this reason, their translation to the clinical setting is dependent upon the development of an efficient delivery system that is able to improve the pharmacokinetic and biodistribution properties of siRNAs.

Recently, engineered designs, such as aptamer-siRNA chimeras and transferring-decorated nanoparticles, have continued to dramatically improve the precision of delivery for RNAi agents[8]. Advances in RNAi-based therapeutics may require new biochemical technologies to maximise drug potency while minimising off-target toxicity and immunogenicity. Meanwhile, we have already reported a novel class of RNAi therapeutic agents (PnkRNA, nkRNA) and evaluated their effectiveness[9]. We showed that PnkRNA and nkRNA directed against transforming growth factor (TGF)-β1 ameliorate outcomes in mouse models of acute lung injury and pulmonary fibrosis. This novel class of RNAi agents was synthesised on solid phase as single-stranded RNAs (ssRNAs) that self-anneal into a unique helical structure containing a central stem and two loops following synthesis (Fig. 1). The production of the novel RNAi agents is simple; because PnkRNA and nkRNA are synthesised as ssRNAs that spontaneously self-anneal, low-cost, large-scale production is possible. These novel RNAi agents have showed significant effectiveness in disease models and also superior resistance against nuclease degradation compared to

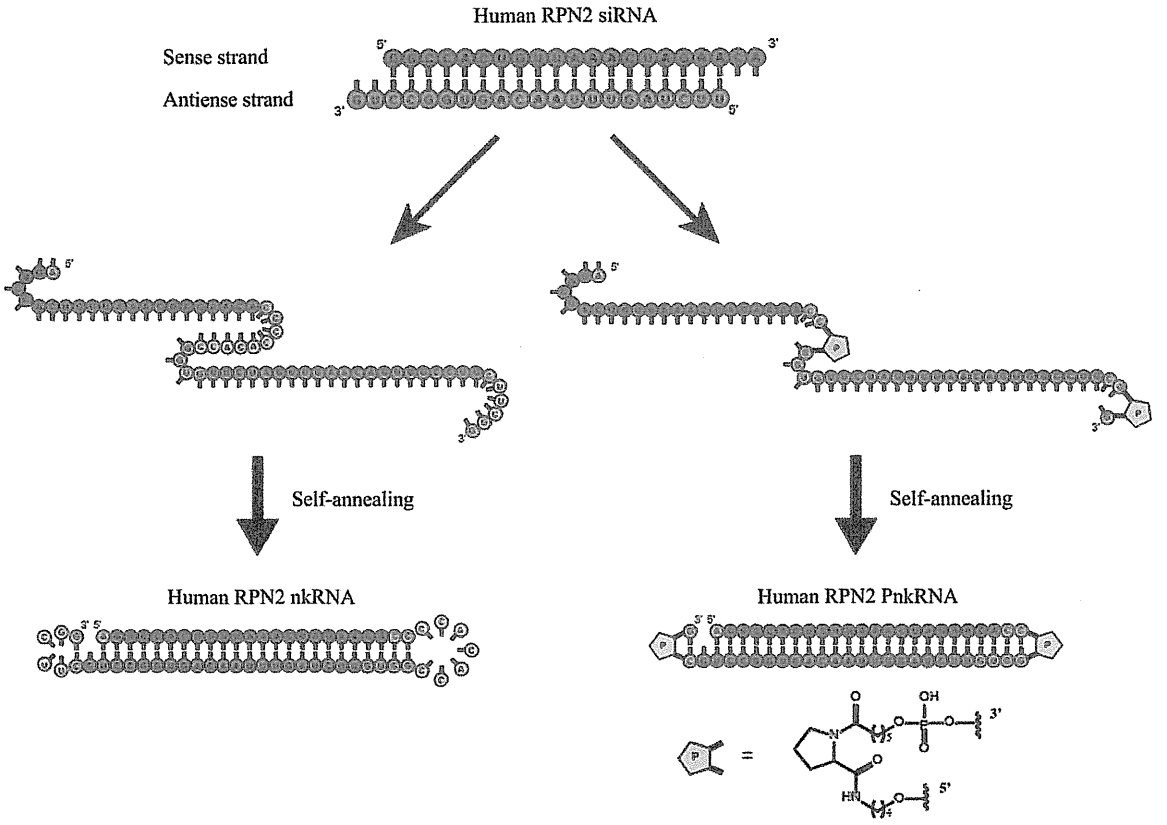

Figure 1 | Structure of novel RNAi agents. Both nkRNA and PnkRNA were prepared as single-stranded RNA oligomers that then self-anneal, as shown. Nucleotides in red indicate the sense strand of the target (RPN2); nucleotides in blue indicate the antisense strand; and nucleotides in green and yellow indicate the loop cassettes. P indicates a proline derivative.

canonical siRNAs. Additionally, by evaluating the induction of proinflammatory cytokines, our previous results suggest that none of the platforms were immunotoxic[9]. Thus, the novel RNAi therapeutic agents are safe and might be employed in clinical applications because they address several issues in siRNA-based therapy.

Lung cancer is the leading cause of cancer-related death in the world. Non-small cell lung cancer (NSCLC) accounts for approximately 85% of all lung cancers. Approximately 70% of all newly diagnosed patients present with local advanced or metastatic disease and require systemic chemotherapy[10,11]. Although NSCLC patients with epidermal growth factor receptor (EGFR) mutations initially respond to EGFR tyrosine kinase inhibitors[12], most patients experience a relapse within 1 year. Despite the development of novel molecular therapies[13], the prognosis of lung cancer is still poor and shows a median survival time of approximately 18 months in the operable stages. Hence, novel and more effective approaches are needed for the treatment of advanced lung cancer. Lung diseases in general are attractive targets for siRNA-based therapeutics because of their lethality and prevalence. In addition, the lung is anatomically accessible to therapeutic agents via the intrapulmonary route. Accessibility is a key requirement for successful RNAi-based *in vivo* and clinical studies, and this characteristic offers several important benefits over systemic delivery, including the use of lower doses of siRNAs, the reduction of undesirable systemic side effects, and improved siRNA stability due to the lower nuclease activity in the airways compared to the serum[14]. The direct administration of siRNAs into the target organs is a promising strategy for overcoming the problems of intravenous administration[15]. On the basis of these promising findings, we explored the effectiveness of this novel class of RNAi therapeutic agents in lung cancer. In the current study, we prepared inhaled novel RNAi agents directed against luciferase and human-ribophorin II (RPN2) as candidate genes, and we compared their inhibitory activity to canonical siRNAs using *in vitro* assays and animal models of lung cancer. Furthermore, using this new technology, lung cancer xenograft studies showed that the aerosol delivery of a naked novel RNAi agent significantly inhibited tumor growth.

Results

***In vitro* stability of novel RNAi agents.** The stability of the novel RNAi agents, PnkRNA and nkRNA, against degradation by ribonucleases was compared with that of siRNA. Each RNAi agent was incubated in the presence of ribonucleases, and the degree of degradation was followed overtime. siRNA was degraded after 5 min of incubation with ribonucleases, but both PnkRNA and nkRNA remained intact after 15 min of incubation (Supplementary Fig. 1). The novel RNAi platforms were more resistant to degradation than siRNA.

Distribution of fluorescent siRNA after inhalation. The inhaled administration of fluorescently labeled siRNA by MicroSprayer™ enabled the efficient intracellular distribution of lung cancer cells throughout the lung parenchyma. The efficient and homogeneous distribution of the RNAi agent to most parts of the lung tissue is a prerequisite for studying target-specific RNAi efficacy. The endotracheal application of suspended RNAi agents by a MicroSprayer™ can result in nanoparticle deposition in smaller airway and peripleural tumor cells (Fig. 2a,b).

Monitoring luciferase inhibition of the inhaled novel RNAi agents' delivery system *in vivo*. Mice with an intravenous injection of

A549-luc-C8 cells on day 0 were imaged twice a week up to day 28. In all mice, measurable lung tumors could be calipered within 2 weeks using this cell line. Four weeks after tumor injection, the observed patterns indicated lesions developing in the lungs of the mice. To estimate whether the aerosol delivery of novel RNAi agents had a valid gene-silencing effect on the lung tumors, the mice were treated with a luciferase siRNA, PnkRNA, and nkRNA, each of which was compared with the control siRNA. The activities of the siRNA and novel RNAi platforms are shown. On the next day, in mice receiving luciferase siRNA and novel RNAi agents, bioluminescence was inhibited by 50–60% in the whole body when compared with bioluminescence before treatment. On the other hand, the bioluminescent signals in the mice that were treated with the control siRNA had increased (Fig. 2c,d). In addition, we found that the RNAi effect of the novel platform would continue for at least five days (supplementary Fig. 2).

***In vitro* suppressive effect of novel RNAi agents for RPN2.** To screen for target genes showing the growth inhibition of A549-luc-C8 cells, RPN2 was selected as a target gene. A549-luc-C8 cells expressed RPN2 mRNA at high levels, as evaluated by real-time RT-PCR, and RPN2 protein expression on immunohistochemical staining was detected in the cytoplasm of cancer cells in the A549-luc-C8 xenograft model (Fig. 3a). To monitor cell growth and

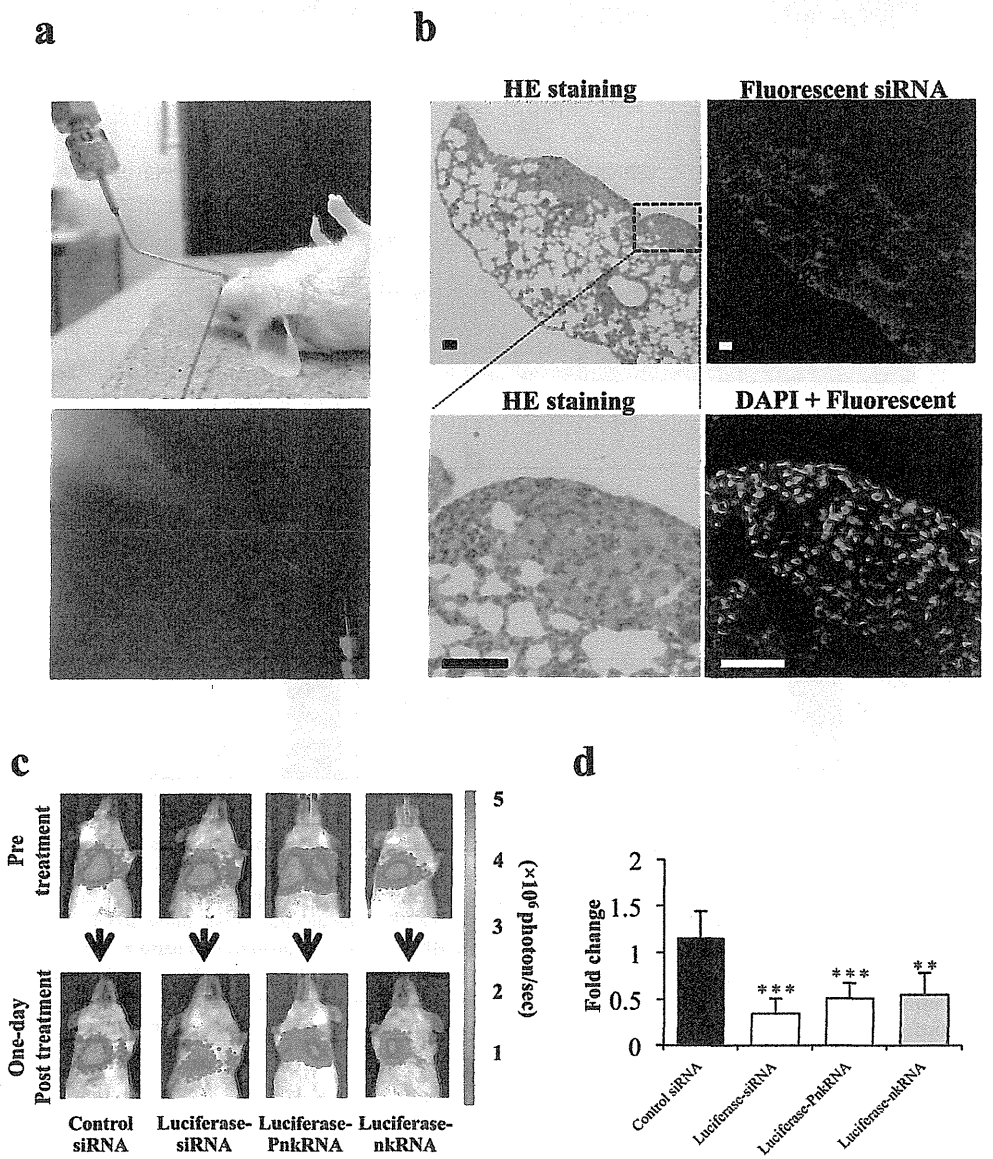

Figure 2 | Inhaled single administration study with novel RNAi platforms against luciferase gene *in vivo*. (a) Intratracheal delivery route: RNAi therapeutic agents are sprayed directly from the mouth into the lungs using a MicroSprayer™ aeroliser. (b) Distribution of fluorescent siRNA in the lungs after inhalation. A sufficient pulmonary distribution of aerosolised siRNA was attained in mice by MicroSprayer™. In addition, intracellular fluorescent staining in lung cancer cells and bronchial epithelial cells was occasionally observed (magnified image, DAPI + Fluorescent siRNA). The scale bars indicate 50 μm. HE, Haematoxylin-eosin. (c) Monitoring luciferase inhibition *in vivo* with bioluminescent imaging. Representative images pre-treatment and on the first day post-treatment. (d) Normalised fold change (one day post-treatment/pre-treatment) of bioluminescence emitted from the whole bodies of mice. The data represent the means ± SD (n = 4). Statistical analysis was performed by the Bonferroni multiple-comparison test. ***, $P < 0.001$ versus control siRNA group. **, $P < 0.01$ versus control siRNA group.

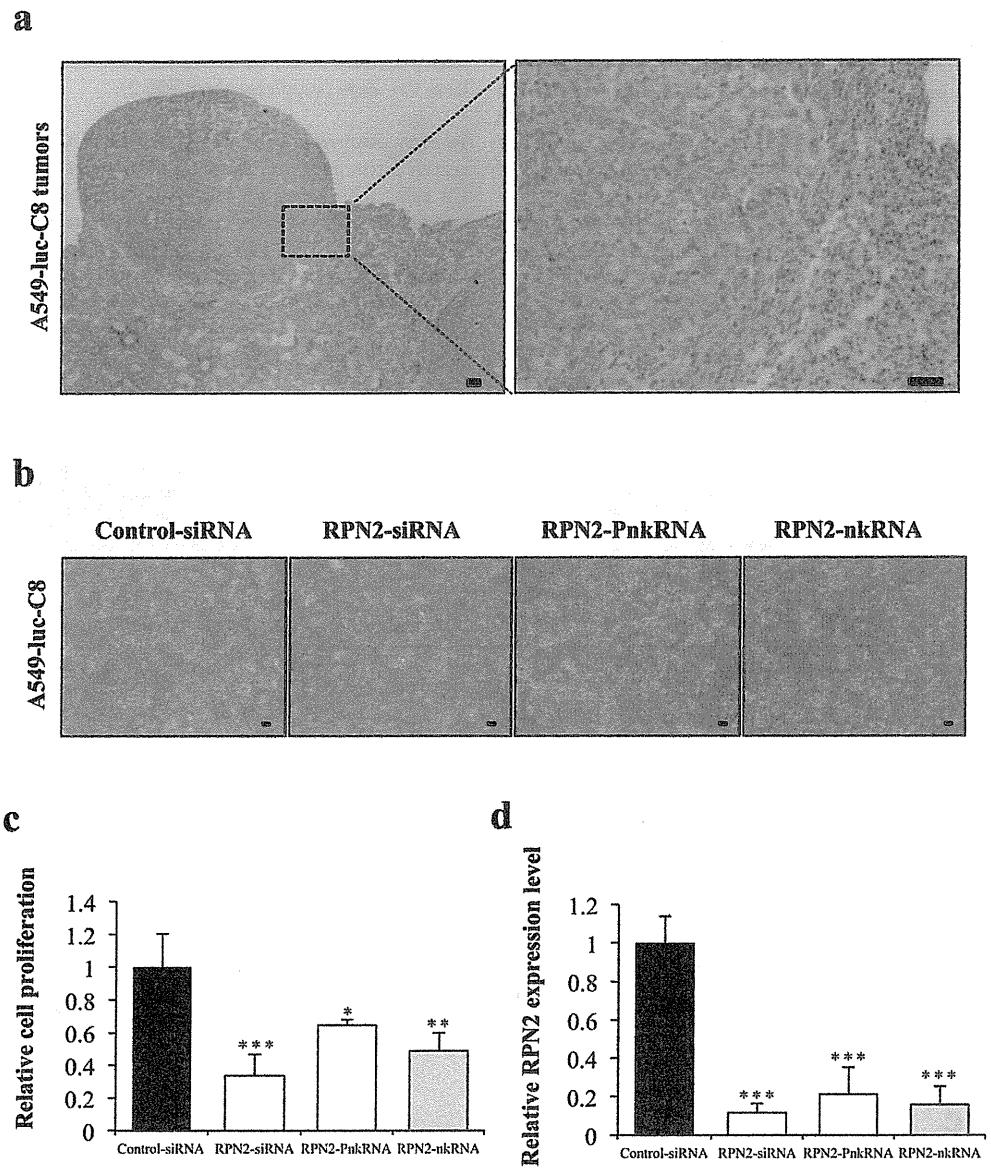

Figure 3 | Suppressive effect of novel RNAi agents for RPN2 in A549-luc-C8 cells. (a) Immunohistochemical staining for RPN2 proteins in representative tumors of A549-luc-C8 xenograft lung cancer models. The scale bars indicate 100 μm. (b) Phase-contrast micrographs of A549-luc-C8 cells 96 h after transfection with RPN2 siRNA, RPN2 PnkRNA, RPN2 nkRNA or control siRNA using DharmaFECT 1 reagent. The scale bars indicate 10 μm. (c) Cell proliferation was measured 96 h after transfection with each of the RNAi therapeutic agents. Inhibition of cell growth was observed on A549-luc-C8 cells treated with RPN2 siRNA, PnkRNA, nkRNA, or the control siRNA. Statistical analysis was performed by the Bonferroni multiple-comparison test. The data represent the means ± SD ($n = 3$). ***, $P < 0.001$ versus control siRNA group. **, $P < 0.01$ versus control siRNA group. *, $P < 0.05$ versus control siRNA group. (d) The inhibition of the targeted mRNA levels is shown. Human RPN2 expression levels were normalised to beta-actin levels. Statistical analysis was performed by the Bonferroni multiple-comparison test. Data represent the means ± SD ($n = 3$). ***, $P < 0.001$ versus control siRNA group.

suppressive effects for RPN2, the RNAi cell transfection method was used. The inhibition of cell growth was observed on A549-luc-C8 cells treated with RPN2 siRNA, PnkRNA, nkRNA, or the control siRNA (Fig. 3b,c). The inhibition of the targeted mRNA levels was also shown (Fig. 3d). RPN2 PnkRNA and nkRNA, as well as siRNA, inhibited A549-luc-C8 cell proliferation and suppressed RPN2 expression. Furthermore, a rescue experiment indicated that exogenous RPN2 expression could rescue the functional changes induced by the specific RNAi knockdown (supplementary Fig. 3a,b). These results revealed that RPN2 may be the target of the inhibition of tumor growth of A549-luc-C8 cells.

Inhibition of RPN2 expression by the inhaled novel RNAi agents' delivery system (single administration study, mice per group; n = 4). To investigate the inhibition of lung cancer by the inhaled novel RNAi agents' delivery system, RPN2 siRNA, PnkRNA and nkRNA were administered intratracheally into mice on day 28 of the intravenous injection of A549-luc-C8 cells. The treatment group

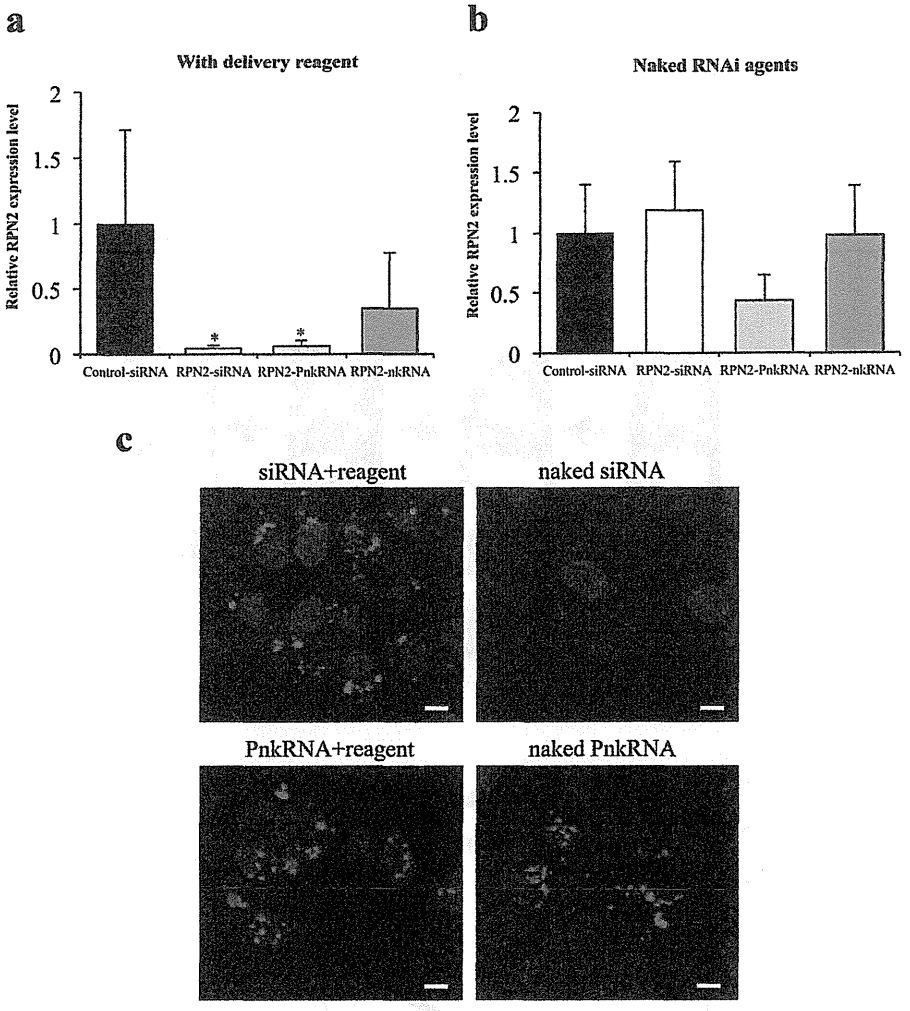

Figure 4 | Single administration study with novel RNAi platforms against RPN2 gene *in vivo* and with an endocytosis assay *in vitro*. The effects of transfection on the expression of RPN2-mRNA 24 h after the inhaled administration of RNAi therapeutic agents with (a) or without delivery reagents (b). Measurements of human RPN2 expression levels by real-time RT-PCR. Data represent the means ± SD ($n = 4$). *, $P < 0.05$ versus control siRNA group. (c) Endocytosis assay for naked RNAi therapeutic agents. Naked PnkRNAs were incorporated into the A549-luc-C8 cell cytoplasm through endocytosis in the absence of delivery reagents. The scale bars indicate 10 μm.

received 15 μg RNAi agent by inhaled administration only on day 28. The total luminescence from all tumors was determined at different times post-treatment until 7 days post-treatment for each mouse. However, there was no suppression of luminescence in mice treated with RPN2 siRNA, PnkRNA, nkRNA, or control siRNA over the same observation period. Upon confirming the down-regulation of RPN2 expression, the xenograft tumor tissues were excised 24 h after the inhaled administration of RNAi agents, and quantitative real-time RT-PCR was performed. RPN2 mRNA was significantly down-regulated in the RPN2 siRNA- and PnkRNA-treated xenografts, compared with those treated with control siRNA (Fig. 4a). Moreover, we also tried to replicate the same inhaled administration study of RNAi agents without delivery vehicles. Remarkably, only naked RPN2-PnkRNA tended to suppress RPN2 mRNA expression, compared with the other three experimental groups (Fig. 4b). The endocytosis assay with labeled siRNAs and PnkRNAs using pHrodo™ Red succinimidyl ester showed the presence of the intracellular fluorescence signal in both A549-luc-C8 cells and PC14 cells transfected with not only RNAi therapeutic agents plus reagent but also naked PnkRNAs (Fig. 4c, Supplementary Fig. 4). This indicates that naked PnkRNAs were incorporated into the cell cytoplasm by endocytosis without delivery reagents. These results suggest that the repeated administration of naked RPN2-PnkRNA might be required for the inhibition of tumor growth. Therefore, we tested the hypothesis that a novel RNAi agent might have emerged as a powerful technology capable of suppressing the expression of target genes without delivery vehicles.

Analysis of the efficiency of naked RPN2-PnkRNA on the inhibition of lung tumor growth (repeated administration study, mice per group; n = 12). Based on the observed PnkRNA pharmacodynamics (supplementary Fig. 2), we believe that the weekly administration schedule of PnkRNA-RPN2 is a reasonable RNAi-therapeutic strategy. To assess the efficiency of the naked novel RNAi (PnkRNA) agent on the inhibition of lung tumor growth, naked RPN2-PnkRNA was intratracheally administered on days 28, 35, and 42 post-inoculation. At the end of the experiment on day 49, mice with naked RPN2-PnkRNA showed inhibition of tumor growth, and there were significant differences between the naked RPN2-PnkRNA and the naked control-PnkRNA on day 49 ($P < 0.05$) (Fig. 5a,b). Histopathological analysis revealed that the

A549-luc-C8 cell lung tumors were significantly inhibited by naked RPN2-PnkRNA (Fig. 5c, d). Furthermore, the lung specimens, including normal lung tissues, did not show any significant toxicity from the aerosol treatment (Fig. 5c). The significant effects did not involve weight loss and were associated with the specific down-regulation of mRNAs and protein at the molecular target (Supplementary Fig. 5a, b). In addition, the number of Ki-67 positive nuclei in naked RPN2-PnkRNA-treated cells was significantly decreased

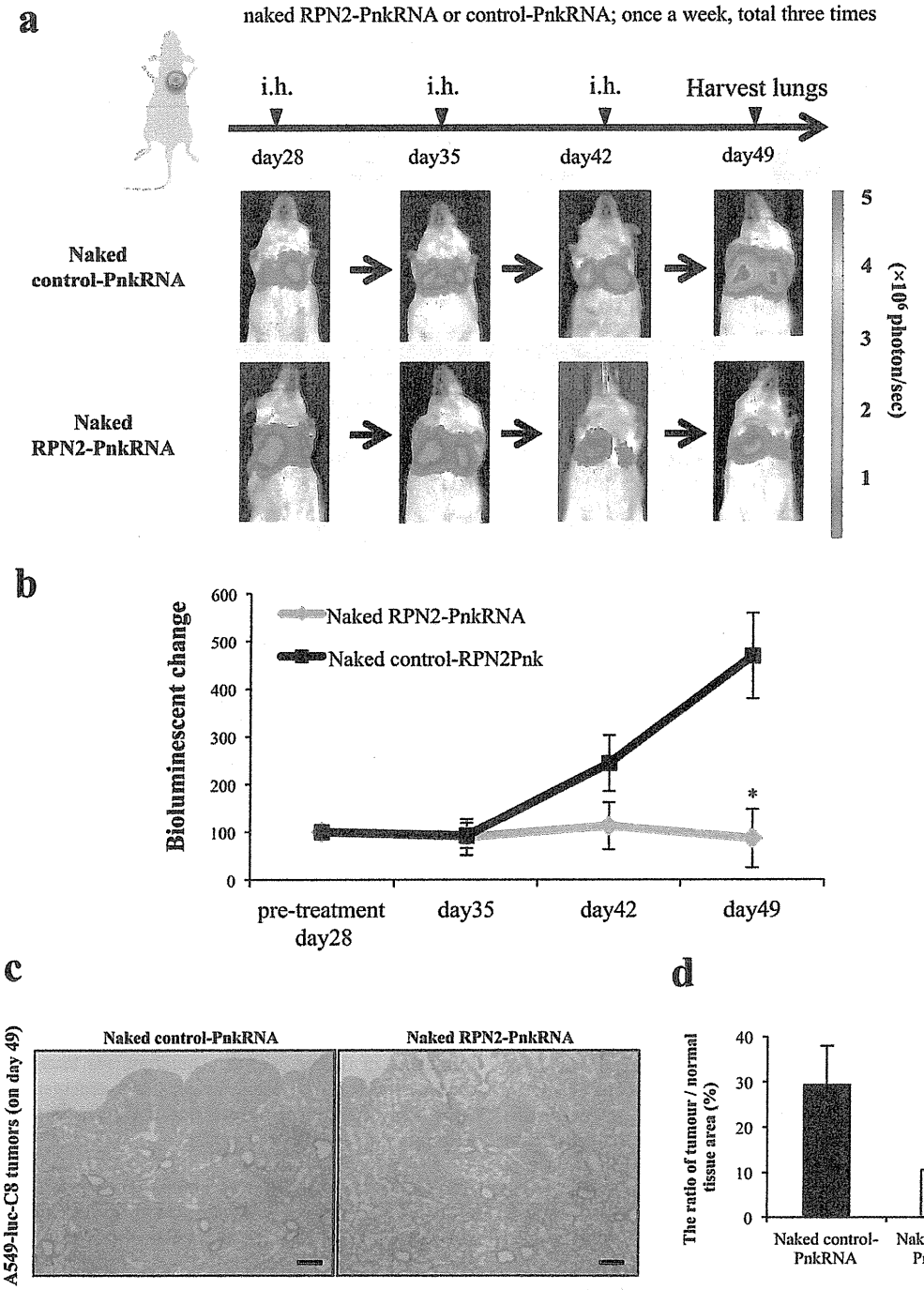

Figure 5 | Repeat administration study with naked RPN2-PnkRNA *in vivo*. (a) Analysis of the efficiency of naked RPN2-PnkRNA upon the inhibition of lung tumor growth after inhaled (i.h.) administration once a week for 3 weeks with bioluminescent imaging. Representative images of scid mice on days 28, 35, 42 and 49. Each experimental regimen consisted of twelve animals. (b) The bioluminescent change (days 35, 42 and 49/pre-treatment day 28) emitted from the whole bodies of the mice on day 28 was set to 100%. Statistical analysis was performed by the Bonferroni multiple-comparison test. The data represent the means ± SD ($n = 12$). *, $P < 0.05$ versus naked control-PnkRNA group. (c) Haematoxylin eosin-stained sections of each of the right lower lobes from the same mice that were imaged in Figure 5a, treated with naked control-PnkRNA or naked RPN2-PnkRNA on day 49. The scale bars indicate 100 μm. (d) The ratio of tumor/normal tissue area (%) of HE staining (on day 49). The data represent the means ± SD (n = 12). Statistical analysis was performed using the Bonferroni multiple-comparison test. *, $P < 0.05$ versus naked control-PnkRNA group.

compared to the control group (Supplementary Fig. 5c). Therefore, the aerosol delivery of naked PnkRNA could be a unique and safe strategy for inhibiting lung cancer growth *in vivo*.

Discussion

Our findings indicate that a novel class of RNAi therapeutic agents (PnkRNA, nkRNA) can be delivered to lung cancer by aerosols. Furthermore, we have demonstrated that a novel RNAi agent, RPN2, markedly suppressed the growth of A549-luc-C8 xenograft tumors *in vivo*. The novel RNAi agent was administered in naked, unmodified form by aerosol. To the best of our knowledge, our results present the first evidence that gene silencing by means of intrapulmonary delivery of naked, unmodified RNAi agents may have therapeutic potential in treating lung cancer. Despite the highly promising potential of RNAi for novel drug discovery, some obstacles still must be overcome before clinical applications[5]. The biggest hurdle remains a suitable delivery method. In this study, we were challenged to overcome this hurdle through a combination of unique RNAi platforms and a local delivery method.

A new class of RNAi agents, PnkRNA and nkRNA, have a unique helical structure containing a central stem and two loops. Their large-scale production at low cost is possible because they do not require an annealing step. Previously, we also reported that the intrapulmonary delivery of novel RNAi agents was not associated with the expression of interferon (IFN)-α or IFN-β in the mouse model of lung diseases, suggesting that they might provide a solution to safety concerns about the off-target effects of canonical siRNAs[9]. In this study, novel RNAi agents showed significant effectiveness in lung cancer xenograft models and proved to be more stable against nuclease degradation than canonical siRNAs. The *in vitro* assay with labeled RNAi therapeutic agents showed that naked PnkRNAs were incorporated into the cell cytoplasm by endocytosis without delivery vehicles; these results were reproduced in two independent lung cancer cell lines. Furthermore, we were successful at providing evidence for this technology by showing that a naked, unmodified PnkRNA significantly inhibited lung tumor growth without any serious toxicity. The naked RNAi therapeutic approach has high safety potential because no proinflammatory or toxicological response was induced by the delivery vehicles. In the specimens of xenograft mouse lungs, no necrosis, degeneration, anaplasia in pneumocytes, atelectasis or emphysema was detected after naked aerosol treatment (Fig. 5c). These data show that naked PnkRNA functions safely and efficiently in an aerosol delivery system. However, we believe that more dedicated studies with aerosol delivery are required to evaluate the possible untoward pulmonary toxicity *in vivo*. In general, naked RNAi agents can avoid many of the issues regarding side effects and toxicities that are related to the formulation of reagents and might be able to facilitate specific therapeutic molecular targeting, which is considered a promising strategy[15,16]. In addition, naked siRNAs can be administered to mice to down-regulate an endogenous or exogenous target without inducing an IFN response[17]. Taken together, strategies using naked novel RNAi agents can be altered to minimise the potential for off-target effects from RNAi therapeutic agents. As one significant limitation of this study, it is unknown whether these novel RNAi-therapeutics would be successful in a host with an intact immune system. We will test the efficacy of naked-PnkRNA delivery technology in immune-competent mice in a future study. Furthermore, we hope that the stability and effectiveness of this technology in humans will be evaluated in preclinical trials.

Dozens of RNAi-based therapeutics are currently undergoing preclinical and clinical trials, and these studies provide further opportunities for successful results[2]. Many of these studies are conducted through local administration to specific tissues, such as ocular, epidermal, pulmonary, colonic, and pancreatic tissues[18]. Thus, the direct-delivery approach can overcome barriers in clinical testing, and successful RNAi can offer high specificity to specific organs and fewer undesirable off-target effects compared to systemic administration[19]. The success of the delivery of RNAi-based therapeutics requires efficiency, convenience, and patient compliance with the delivery route. For these reasons, the aerosol delivery system of RNAi agents is a safe and powerful potential treatment for lung cancer; because the anatomical structure and location of the lungs make this simple, non-invasive approach possible and its high delivery efficiency reduces systemic side effects. Here, we provided evidence that the aerosol delivery of a naked, unmodified RNAi agent by the MicroSprayer™ technique results in a highly improved local distribution in the lung peripheries. Although further analysis is required, our novel technology delivered by aerosol can be altered to minimise the potential for off-target effects from RNAi therapeutic agents.

The potency and target specificity of the RNAi knockdown have generated considerable excitement as a new therapeutic modality for cancer therapy. There have already been significant improvements in RNAi-based therapeutics for the treatment of various cancers, including lung cancer[20]. Honma *et al* revealed that RPN2, which is part of an N-oligosaccharyltransferase complex, efficiently induced apoptosis in docetaxel-resistant human breast cancer cells[21]. Recently, RPN2 expression has also been shown to be a potential therapeutic target and promising prognostic marker for several types of cancer[22,23]. Remarkably, Zhu *et al* revealed that RPN2 is highly expressed in $CD24^{+}CD44^{+}$ stem-like pancreatic cancer cells[22]. We have also recently demonstrated that RPN2 is multifunctional, that it tightly regulates tumor survival, and that it is anti-apoptotic. RPN2 regulates cancer stem cell properties through the stabilization of mutant p53. Furthermore, RNAi-mediated knockdown in several types of cancer cells results in cell growth inhibition *in vitro* and *in vivo*[24]. These findings suggest that RPN2 could be a promising therapeutic target for several types of cancer. The data presented in this study demonstrate that the expression of RPN2 is involved in lung tumor growth *in vitro* and in lung cancer xenograft models. Furthermore, based on a rescue experiment, exogenous RPN2 expression can rescue the functional changes induced by specific RNAi knockdown. Therefore, our study indicated that RPN2 might serve as a potential target for gene therapy in lung cancer treatment. Although RPN2 RNAi agents efficiently inhibited the proliferation of A549-luc-C8 cells, further study is required to develop an RNAi-based therapy that induces cytocidal activity specific to the lung cancer cells. It would be worthwhile to investigate in a future study whether naked RPN2-PnkRNA treatment combined with docetaxel is a better therapeutic strategy against lung cancer.

A major limitation of this study is that it is entirely based on a single cell line, a single target. Non–small cell lung cancers (NSCLCs) harbor a single specific mutated oncogene like K-ras that is thought to be the primary genetic "driver" leading to lung cancer. In this experiment, we used mutant k-ras cell line and still do not know the RPN2 function is mutant k-ras-dependent phenotype or not. Therefore, we plan to utilize a naked RNAi-based therapeutic technology in other lung cancer cell lines and other gene targets to establish delivery efficacy in future studies.

In conclusion, we have developed a new technology with unique RNAi platforms delivered by aerosol. Our findings have provided new insights into the availability of naked and unmodified RNAi agents in RNAi therapeutic trials. These novel findings also have the potential to make an extremely valuable contribution to the development of lung cancer treatment as a reasonable class of RNAi-based therapy.

Methods

Reagents. The antibiotic solution (containing 10,000 U/mL penicillin and 10 mg/mL streptomycin), the trypsin-EDTA mixture (containing 0.05% trypsin and EDTA), RPMI-1640, FBS (foetal bovine serum) and pHrodo™ Red succinimidyl ester were

obtained from Invitrogen (Carlsbad, CA). The pairs of each small interfering RNA (siRNA) and novel RNAi reagent, targeting luciferase mRNA, and human RPN2 mRNA (Supplementary Table 1, 2) were purchased from Bonac (Kurume, Japan). Allstars Negative Control siRNA was obtained from Qiagen (Hilden, Germany).

Preparation of novel RNAi agents. The preparation of proline diamide amidite and the novel RNAi agents has been previously described[9]. Novel RNAi agents are prepared as single-stranded RNA that self-anneals into a unique structure containing a double-stranded RNA with an unpaired site bound at the right and left ends by an oligonucleotide loop or by a non-nucleotide molecule (a proline derivative). Fig. 1 shows the schematic model of human RPN2, which was selected as a representative RNAi target.

RNA stability. To estimate the resistance to nucleases, 40 μl (2 μmol/l) of siRNA, nkRNA and PnkRNA directed against human RPN2 were incubated at 37°C with 1 μl of RNase Cocktail Enzyme Mix (Ambion, Foster City, CA) (RNase A 500 U/ml, RNase T1 20,000 U/ml). After the specified times, the ribonuclease reaction was stopped, and 2 μl of each sample was run on 3% agarose gel.

Cell line. A549-luc-C8 cells, a luciferase-expressing cell line derived from A549 human lung adenocarcinoma cells by stable transfection of the North American Firefly Luciferase gene expressed from the CMV promoter, were purchased from Xenogen. The human lung adenocarcinoma cell line PC14 was obtained from RIKEN BioResource Center (Tokyo, Japan). These cells were cultured in RPMI-1640 containing 10% heat-inactivated FBS and an antibiotic-antimycotic at 37°C in 5% CO_2.

RNA extraction. Total RNA was extracted from cultured cells or mice lungs using QIAzol and miRNeasy Mini Kit (Qiagen) according to the manufacturer's protocol. The purity and concentration of all RNA samples were quantified using NanoDrop ND-1000 (Thermo Scientific, San Jose, CA). For RPN2 mRNA analysis of mice lungs, the animals were sacrificed 24 h after the inhaled administration of each RNAi agent.

Quantitative Real-time PCR (qRT-PCR). The reverse transcription reaction was performed with a High-Capacity cDNA Reverse Transcription Kit (Applied Biosystems, Foster City, CA) using a random hexamer primer. The synthesised cDNAs were quantified by SYBR Green I qRT-PCR. Quantitative real-time reverse transcription-PCR (qRT-PCR) analysis was conducted using primers for human RPN2 (forward:5′-CTTCCAGAGCCACTGTCCTC-3′; reverse: 5′-CCGGTTGTC-ACCTTCAACTT-3′). β-Actin (forward:5′-ATTGCCGACAGGATGCAGA-3′; reverse:5′-GAGTACTTGCGCTCAGGAGGA-3′) was used for normalisation. The relative amounts of RPN2 were measured using the 2(-Delta Delta C(T)) method. The reactions were performed with the ABI Prism 7300 Sequence Detection System (Applied Biosystems) at 95°C/10 min, followed by 40 cycles at 95°C/15 s and 60°C/30 s. All qRT-PCR reactions were performed in triplicate.

Transient transfection assays. A549-luc-C8 cells were plated on six-well plates at a density of 2×10^5 cells/well and grown overnight until 50–80% confluence was achieved to obtain maximum transfection efficiency. The cells were transfected with validated siRNA, the novel RNAi agents (PnkRNA, nkRNA) for RPN2, or Allstars Negative Control siRNA (Qiagen) at a final concentration of 25 nmol/l using the DharmaFECT 1 reagent (Thermo Scientific), according to the manufacturer's protocol. In the cDNA rescue experiment, an RPN2 Human cDNA ORF clone (Origene Technologies, Rockville, MD) or pEGFP-N1 (Clontech Laboratories, Mountain View, CA) was combined with each siRNA using DharmaFECT Duo (Thermo Scientific), according to the manufacturer's protocol. RPN2-siRNA targeting site is located 906 nt downstream of the ATG start codon of human RPN2 cDNA sequence on human RPN2 expression vector.

Cell Proliferation Assay (MTS assay). A Cell Counting Kit-8 (CCK-8) (Dojindo Laboratories, Kumamoto, Japan) was used in the cell proliferation assay. Five thousand cells per well were seeded in 96-well plates. The following day, the cells were replenished with fresh medium containing 25 nmol/l of each RNAi agent. After four days of culture, a plate was assayed by adding 10 μl of CCK-8 solution to each well, and the plate was further incubated for 4 h at 37°C. The absorbance at 450 nm was measured using Envision (PerkinElmer, Norwalk, CT).

RNAi therapeutic agent labelling with pHrodo™ Red succinimidyl ester and endocytosis assay. The fluorescence of the pHrodo™ Red dye increases as the pH decreases from neutral to acidic, making it an ideal tool to study endocytosis[25]. The amine-reactive forms of pHrodo™ Red succinimidyl ester were used for labelling the RNAi therapeutic agents. After being labeled according to the manufacturer's protocol, the oligonucleotides were purified by reverse-phase HPLC. A549-luc-C8 cells or PC14 cells were transfected with the labeled siRNAs or PnkRNAs. Each labeled oligonucleotide was transfected with or without DharmaFECT 1 reagent. Then, the plates were incubated at 37°C for 3 hours to allow endocytosis to run to completion. Hoechst 33342 was used as a DNA counter-stain (cyan). Microscopic analysis was performed with a FLUOVIEW FV10i confocal microscope.

***In vivo* imaging of RNAi therapeutic agents in mice with lung cancer.** Animal experiments were performed in compliance with the guidelines of the Institute for Laboratory Animal Research, National Cancer Center Research Institute. These studies were approved by the National Cancer Center Research Institute. Six- to seven-week-old male C.B-17/Icr-scid/scidJcl mice (CLEA Japan, Shizuoka, Japan) were used in the experiments. The animals were housed in a 12 h light/12 h dark cycle and provided with an autoclaved rodent diet and water *ad libitum*. The mice were injected intravenously with 2×10^6 A549-luc-C8 cells suspended in 0.25 ml of sterile Dulbecco's PBS via the tail vein (day 0). For *in vivo* imaging, the mice were administered 150 mg/kg D-luciferin (Promega, Madison, WI) by intraperitoneal injection. Ten minutes later, photons from the whole bodies of the animals were counted by measuring bioluminescence with an IVIS imaging system (Xenogen, Alameda, CA), according to the manufacturer's instructions. The data were analysed using LIVINGIMAGE 4.2 software (Xenogen). The development of lung cancer was monitored twice a week *in vivo* by bioluminescent imaging. Four weeks after tumor injection (day 28), the bioluminescence from the implanted cancer cells was measured, and the mice were divided into four treatment groups (single administration study, mice per group; n = 4) or two groups (repeated administration study, mice per group; n = 12) with equivalent levels of bioluminescence. In the single administration study, the individual mice were administered 15 μg of each RNAi agent with *In vivo*-jetPEI™ (Polyplus Transfection Inc, New York, NY) (resulting in a calculated 1 : 6 charge ratio of nucleic acid backbone phosphates to cationic lipid nitrogen atoms) in a volume of 25 μl on day 28 using an endotracheally inserted MicroSprayer™ aerosoliser (IA-1C; Penn-Century) and a high-pressure syringe (FMJ-250; Penn-Century, Philadelphia, PA)[26]. Data are from a representative experiment of three independent experiments. In the repeated administration study, the treatment—15 μg of each naked RNAi agent inhaled by using a MicroSprayer™ aerosoliser—was performed on days 28, 35, and 42 (once a week for 3 weeks, three treatments total). To control for mouse-to-mouse variability, the bioluminescence ratio for each mouse was normalised by dividing by each day of the post-treatment/pre-treatment (day28) ratio of luciferase intensity for that mouse. For *in vivo* knockdown analysis, animals were sacrificed 24 h after each RNAi application, and lungs were removed and processed for histology or knockdown determination by qRT-PCR (SYBR Green).

Lung histological findings. Lung tissues were fixed in 10% neutral buffered formalin, paraffin-processed, and sectioned at 5 μm. Formalin-fixed and paraffin-embedded slides were stained with haematoxylin and eosin (H&E) or used for immunohistochemical (IHC) staining. With regard to the histologic estimation of tumor burden, the freeware *Image J* (National Institutes of Health, Bethesda, Maryland, USA) was used. Upon the IHC staining, antigen retrieval was performed by autoclave in a 10 mmol/l sodium citrate buffer (pH 6.0), and the endogenous peroxidase activity was blocked with the Immuno Pure Peroxidase Suppressor (Pierce, Chester, UK). The slides were incubated with RPN2 (A-1, Santa Cruz Biotechnology, Santa Cruz, CA) or Ki-67 (M7240, Dako Cytomation, Copenhagen, Denmark) primary antibody at 4°C overnight. The next day, after washing, the samples were incubated with mouse peroxidase-conjugated anti-mouse IgG (ImmPRESS Reagent; Vector Labs, Burlingame, CA) for 1 h. The immunoreactions were visualised with diaminobenzidine, and the sections were counterstained with haematoxylin.

Immunofluorescence staining. To estimate the inhaled distribution of RNAi agents, 15 μg of Allstars NegativesiRNA Alexia Fluor 647 (Qiagen) with *In vivo*-jetPEI™ was aerosolised by means of a MicroSprayer™, and the lungs were harvested 6 h after application, processed for paraffin sectioning, and analysed by confocal microscopy. DAPI staining was carried out immediately before imaging. Imaging for the cyan (DAPI) and magenta (fluorescently labeled siRNA) channels was performed in sequential mode using the appropriate excitation and emission settings. Microscopic analysis was performed with a FLUOVIEW FV10i confocal microscope (OLYMPUS, Tokyo, Japan).

Statistical analysis. All experiments were repeated at least three times, and the results are expressed as the means ± SE. The statistical analyses were conducted using the Bonferroni multiple-comparison test. These analyses were performed with the Expert StatView analysis software (version 4; SAS Institute, Cary, NC). $P < 0.05$ was considered to be statistically significant.

1. Matranga, C., Tomari, Y., Shin, C., Bartel, D. P. & Zamore, P. D. Passenger-strand cleavage facilitates assembly of siRNA into Ago2-containing RNAi enzyme complexes. *Cell* **123**, 607–620 (2005).
2. Davidson, B. L. & McCray, P. B., Jr. Current prospects for RNA interference-based therapies. *Nat Rev Genet* **12**, 329–340 (2011).
3. Takeshita, F. & Ochiya, T. Therapeutic potential of RNA interference against cancer. *Cancer Sci* **97**, 689–696 (2006).
4. Kim, D. H. & Rossi, J. J. Strategies for silencing human disease using RNA interference. *Nat Rev Genet* **8**, 173–184 (2007).
5. Pecot, C. V., Calin, G. A., Coleman, R. L., Lopez-Berestein, G. & Sood, A. K. RNA interference in the clinic: challenges and future directions. *Nat Rev Cancer* **11**, 59–67 (2011).
6. Chernolovskaya, E. L. & Zenkova, M. A. Chemical modification of siRNA. *Curr Opin Mol Ther* **12**, 158–167 (2010).
7. Lares, M. R., Rossi, J. J. & Ouellet, D. L. RNAi and small interfering RNAs in human disease therapeutic applications. *Trends Biotechnol* **28**, 570–579 (2010).

8. Zhou, J., Bobbin, M. L., Burnett, J. C. & Rossi, J. J. Current progress of RNA aptamer-based therapeutics. *Front Genet* **3**, 234 (2012).
9. Hamasaki, T. *et al.* Efficacy of a novel class of RNA interference therapeutic agents. *PLoS One* **7**, e42655 (2012).
10. Molina, J. R., Yang, P., Cassivi, S. D., Schild, S. E. & Adjei, A. A. Non-small cell lung cancer: epidemiology, risk factors, treatment, and survivorship. *Mayo Clin Proc* **83**, 584–594 (2008).
11. Ramalingam, S. S., Owonikoko, T. K. & Khuri, F. R. Lung cancer: New biological insights and recent therapeutic advances. *CA Cancer J Clin* **61**, 91–112 (2011).
12. Herbst, R. S., Heymach, J. V. & Lippman, S. M. Lung cancer. *N Engl J Med* **359**, 1367–1380 (2008).
13. Pao, W. & Girard, N. New driver mutations in non-small-cell lung cancer. *Lancet Oncol* **12**, 175–180 (2011).
14. Agu, R. U., Ugwoke, M. I., Armand, M., Kinget, R. & Verbeke, N. The lung as a route for systemic delivery of therapeutic proteins and peptides. *Respir Res* **2**, 198–209 (2001).
15. Lam, J. K., Liang, W. & Chan, H. K. Pulmonary delivery of therapeutic siRNA. *Adv Drug Deliv Rev* **64**, 1–15 (2012).
16. Morin, A., Gallou-Kabani, C., Mathieu, J. R. & Cabon, F. Systemic delivery and quantification of unformulated interfering RNAs in vivo. *Curr Top Med Chem* **9**, 1117–1129 (2009).
17. Heidel, J. D., Hu, S., Liu, X. F., Triche, T. J. & Davis, M. E. Lack of interferon response in animals to naked siRNAs. *Nat Biotechnol* **22**, 1579–1582 (2004).
18. Burnett, J. C. & Rossi, J. J. RNA-based therapeutics: current progress and future prospects. *Chem Biol* **19**, 60–71 (2012).
19. Schlee, M., Hornung, V. & Hartmann, G. siRNA and isRNA: two edges of one sword. *Mol Ther* **14**, 463–470 (2006).
20. Petrocca, F. & Lieberman, J. Promise and challenge of RNA interference-based therapy for cancer. *J Clin Oncol* **29**, 747–754 (2011).
21. Honma, K. *et al.* RPN2 gene confers docetaxel resistance in breast cancer. *Nat Med* **14**, 939–948 (2008).
22. Zhu, J., He, J., Liu, Y., Simeone, D. M. & Lubman, D. M. Identification of glycoprotein markers for pancreatic cancer CD24+CD44+ stem-like cells using nano-LC-MS/MS and tissue microarray. *J Proteome Res* **11**, 2272–2281 (2012).
23. Kurashige, J. *et al.* RPN2 expression predicts response to docetaxel in oesophageal squamous cell carcinoma. *Br J Cancer* **107**, 1233–1238 (2012).
24. Takahashi, R. *et al.* Ribophorin II regulates breast tumor initiation and metastasis through the functional suppression of GSK3β. *Sci. Rep.* **3**, 2474; doi:10.1038/srep02474 (2013).
25. Han, J. & Burgess, K. Fluorescent indicators for intracellular pH. *Chem Rev* **110**, 2709–2728 (2010).
26. Bivas-Benita, M., Zwier, R., Junginger, H. E. & Borchard, G. Non-invasive pulmonary aerosol delivery in mice by the endotracheal route. *Eur J Pharm Biopharm* **61**, 214–218 (2005).

Acknowledgments

This work was supported in part by a grant-in-aid for the Third-Term Comprehensive 10-Year Strategy for Cancer Control of Japan; Project for Development of Innovative Research on Cancer Therapeutics (P-Direct); Scientific Research on Priority Areas Cancer, Scientific Research on Innovative Areas ("functional machinery for non-coding RNAs") from the Japanese Ministry of Education, Culture, Sports, Science, and Technology; the National Cancer Center Research and Development Fund (23-A-2, 23-A-7, 23-C-6,); the Program for Promotion of Fundamental Studies in Health Sciences of the National Institute of Biomedical Innovation (NiBio), the Project for Development of Innovative Research on Cancer Therapeutics; and the Japan Society for the Promotion of Science (JSPS) through the "Funding Program for World-Leading Innovative R&D on Science and Technology (FIRST Program)" initiated by the Council for Science and Technology Policy (CSTP). We thank Ayako Inoue and Maki Abe for her excellent technical assistance.

Author contributions

T. Ochiya and K.K. conceived the idea and coordinated the project. Y.F. performed a significant amount of the experimental work. T. Ochiya, Y.F., F.T., T.M. and T. Ohgi wrote the manuscript and prepared the figures and tables. In vivo experiments were carried out by Y.F. and F.T.

Additional information

Supplementary information accompanies this paper at http://www.nature.com/scientificreports

Competing financial interests: The authors declare no competing financial interests.

How to cite this article: Fujita, Y. *et al.* A novel platform to enable inhaled naked RNAi medicine for lung cancer. *Sci. Rep.* **3**, 3325; DOI:10.1038/srep03325 (2013).

Research article

Myelodysplastic syndromes are induced by histone methylation–altering *ASXL1* mutations

Daichi Inoue,[1] Jiro Kitaura,[1] Katsuhiro Togami,[1] Koutarou Nishimura,[1] Yutaka Enomoto,[1] Tomoyuki Uchida,[1] Yuki Kagiyama,[1] Kimihito Cojin Kawabata,[1] Fumio Nakahara,[1] Kumi Izawa,[1] Toshihiko Oki,[1,2] Akie Maehara,[1] Masamichi Isobe,[1] Akiho Tsuchiya,[1] Yuka Harada,[3] Hironori Harada,[4] Takahiro Ochiya,[5] Hiroyuki Aburatani,[6] Hiroshi Kimura,[7] Felicitas Thol,[8] Michael Heuser,[8] Ross L. Levine,[9] Omar Abdel-Wahab,[9] and Toshio Kitamura[1,2]

[1]Division of Cellular Therapy, Advanced Clinical Research Center, and [2]Division of Stem Cell Signaling, Center for Stem Cell Biology and Regenerative Medicine, Institute of Medical Science, University of Tokyo, Tokyo, Japan. [3]Division of Radiation Information Registry and [4]Department of Hematology and Oncology, Research Institute for Radiation Biology and Medicine, Hiroshima University, Hiroshima, Japan. [5]Division of Molecular and Cellular Medicine, National Cancer Center Research Institute, Tokyo, Japan. [6]Genome Science Division, Research Center for Advanced Science and Technology, University of Tokyo, Tokyo, Japan. [7]Graduate School of Frontier Biosciences, Osaka University, Osaka, Japan. [8]Department of Hematology, Hemostasis, Oncology, and Stem Cell Transplantation, Hannover Medical School, Hannover, Germany. [9]Human Oncology and Pathogenesis Program and Leukemia Service, Department of Medicine, Memorial Sloan-Kettering Cancer Center, New York, New York, USA.

Recurrent mutations in the gene encoding additional sex combs-like 1 (*ASXL1*) are found in various hematologic malignancies and associated with poor prognosis. In particular, *ASXL1* mutations are common in patients with hematologic malignancies associated with myelodysplasia, including myelodysplastic syndromes (MDSs), and chronic myelomonocytic leukemia. Although loss-of-function *ASXL1* mutations promote myeloid transformation, a large subset of *ASXL1* mutations is thought to result in stable truncation of ASXL1. Here we demonstrate that C-terminal–truncating *Asxl1* mutations (ASXL1-MTs) inhibited myeloid differentiation and induced MDS-like disease in mice. ASXL1-MT mice displayed features of human-associated MDS, including multilineage myelodysplasia, pancytopenia, and occasional progression to overt leukemia. ASXL1-MT resulted in derepression of homeobox A9 (*Hoxa9*) and microRNA-125a (miR-125a) expression through inhibition of polycomb repressive complex 2–mediated (PRC2-mediated) methylation of histone H3K27. miR-125a reduced expression of C-type lectin domain family 5, member a (*Clec5a*), which is involved in myeloid differentiation. In addition, HOXA9 expression was high in MDS patients with ASXL1-MT, while *CLEC5A* expression was generally low. Thus, ASXL1-MT–induced MDS-like disease in mice is associated with derepression of *Hoxa9* and miR-125a and with *Clec5a* dysregulation. Our data provide evidence for an axis of MDS pathogenesis that implicates both ASXL1 mutations and miR-125a as therapeutic targets in MDS.

Introduction

Additional sex combs-like 1 (*ASXL1*) is 1 of 3 mammalian homologs of the Drosophila *additional sex combs* (*Asx*), and plays critical roles both in activation and suppression of *Hox* genes in axial patterning through regulating the polycomb group and trithorax group proteins (1–4). *ASXL1* is mutated in patients with the entire spectrum of myeloid malignancies including 11%–21% of patients with myelodysplastic syndrome (MDS) (5–8), 10%–15% of patients with myeloproliferative neoplasms (MPNs), 5%–25% of patients with acute myeloid leukemia (AML) (5, 7), and 43%–58% of patients with chronic myelomonocytic leukemia (CMML) (6, 7, 9, 10). Additionally, *ASXL1* mutations are associated with adverse survival in a variety of myeloid malignancies (8, 9).

Recently it was reported that ASXL1 binds members of the polycomb repressive complex 2 (PRC2), specifically EZH2, EED, and SUZ12, and that ASXL1 loss in myeloid hematopoietic cells profoundly inhibits trimethylation of histone H3–lysine 27 (H3K27me3), a hallmark repressive modification induced by the PRC2 (11). ASXL1 also associates with the deubiquitinating enzyme BAP1, which may promote expression of genes (12) through removal of H2A lysine 119 ubiquitination placed by the PRC1 complex. Thus, ASXL1 appears to be involved in both PRC2-mediated gene repression and opposition of PRC1 function (13).

Although loss of ASXL1 promotes myeloid transformation by impairing PRC2-mediated gene repression at a number of critical loci (11), intriguingly, most *ASXL1* mutations are located in the 5′ region of the last exon (exon 12), which are predicted to result in expression of a truncated ASXL1 protein. As further support for this, *ASXL1* mutations are usually heterozygous, leaving 1 allele intact. Therefore, we hypothesized that the C-terminal truncated form of ASXL1 might function as a dominant-negative mutant that suppresses the ASXL1-WT function or alternatively as a gain-of-function mutant (14, 15). These possible effects of *ASXL1* mutations have not been studied and are critical to delineate given the clinical importance of *ASXL1* mutations.

In this study we show that *ASXL1* mutations profoundly inhibited myeloid differentiation in vitro and induced typical MDS in a mouse model. We then sought to explore the molecular link between *ASXL1* mutations and epigenetic disturbances that lead to development of MDS. We identify that expression of mutant forms of ASXL1 results in impaired PRC2 function and impaired myeloid differentiation in vitro and in vivo. Moreover, we identify that *ASXL1* mutations induce upregulated expres-

Conflict of interest: The authors have declared that no conflict of interest exists.
Citation for this article: *J Clin Invest.* 2013;123(11):4627–4640. doi:10.1172/JCI70739.

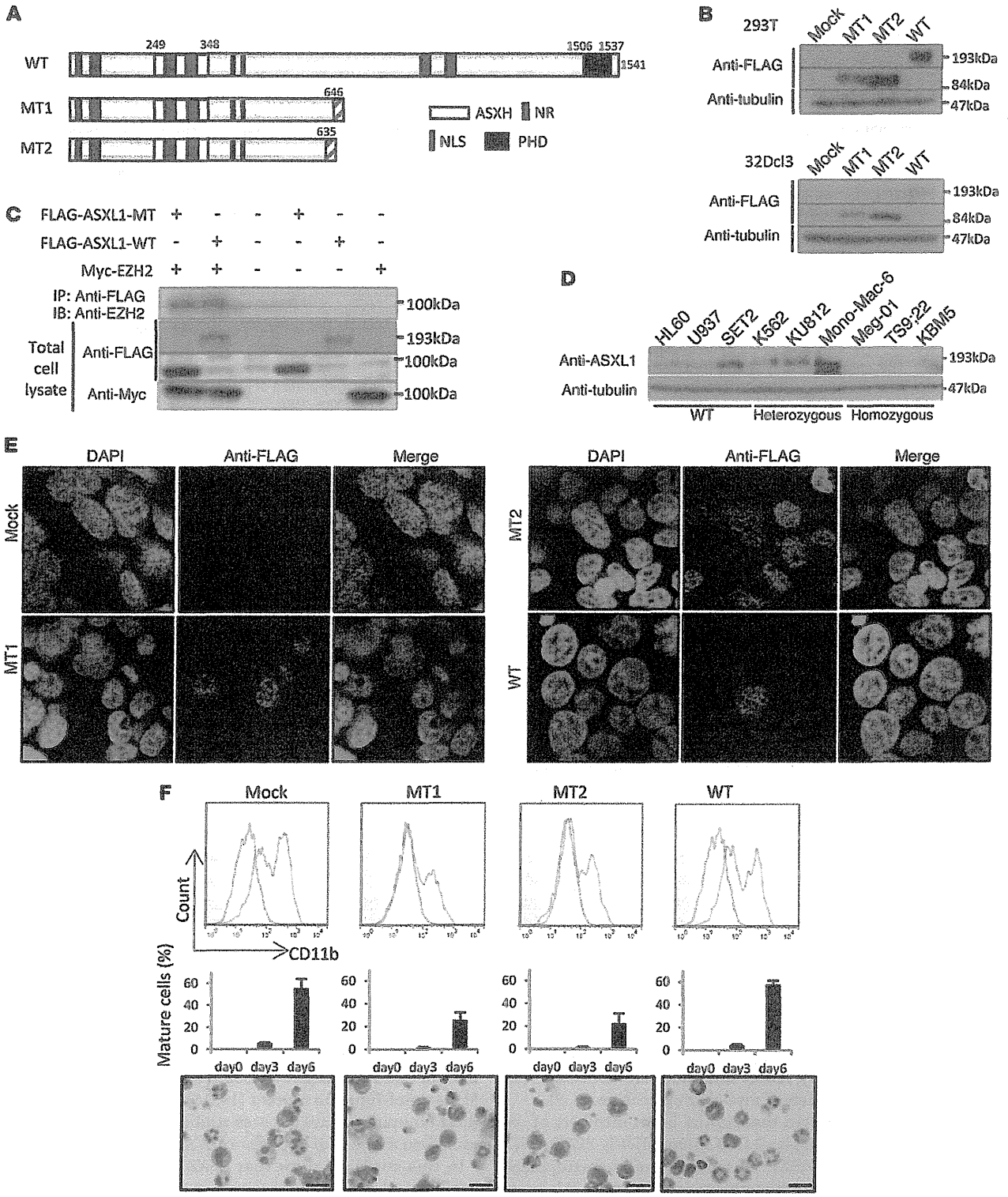

Figure 1
ASXL1 mutations inhibit G-CSF–induced myeloid differentiation of 32Dcl3 cells. (**A**) Schematic diagram of ASXL1-WT and 2 mutants, ASXL1-MT1 and ASXL1-MT2. ASXH, ASX homology region; NLS, nuclear localization signal; NR, putative nuclear receptor coregulator binding motifs; PHD, plant homeodomain. (**B**) Expression of ASXL1-WT and its mutants in 293T cells or 32Dcl3 cells transiently transfected or stably transduced with a FLAG-ASXL1-MT1, ASXL1-MT2, ASXL1-WT, or an empty vector (pMYs-IG). (**C**) HEK293T cells were transiently transfected with FLAG-ASXL1-MT, FLAG-ASXL1-WT, and Myc-EZH2 cDNA, followed by IP of FLAG epitope and Western blotting for EZH2. Cell lysates were also subject to immunoblotting with anti-FLAG Ab or anti-Myc Ab. (**D**) ASXL1 protein expression using C-terminus anti-ASXL1 antibodies in leukemia cell lines. Harboring mutations are as follows: K562, heterozygous *ASXL1* Y591Y/X; KU812, heterozygous *ASXL1* R693R/X; Mono-Mac-6, heterozygous *ASXL1* L1393RfsX30; MEG-01, homozygous *ASXL1* G646WfsX12; TS9:22, homozygous *ASXL1* R693X; KBM5, homozygous *ASXL1* G710X. (**E**) Nuclear localization of ASXL1-MTs. The 293T cells transiently transfected with pMYs-IG, pMYs-FLAG-ASXL1-MT1-IG, pMYs-FLAG-ASXL1-MT2-IG, or pMYs-FLAG-ASXL1-WT-IG were immunostained with anti-FLAG Ab (red) and DAPI (blue). Original magnification, ×600. (**F**) Surface expression of CD11b in 32Dcl3 cells transduced with indicated plasmid after incubation with 1 ng/ml IL-3 (blue) or 50 ng/ml G-CSF for 6 days (red) was analyzed by flow cytometry (top). Filled histograms show control (IgG). Proportions of segmented cells on days 0, 3, and 6 of G-CSF stimulation are shown (middle). Morphology of the cells 6 days after G-CSF stimulation was assessed by Wright-Giemsa staining (bottom). Original magnification, ×400; scale bars: 20 μm.

sion of microRNA-125a (miR-125a) and subsequent suppression of *C-type lectin domain family 5, member a* (*Clec5a*), a type II membrane protein critical for myeloid differentiation. These results identify what we believe is a novel genetically accurate murine model of MDS and additional critical pathways for *ASXL1*-mediated myeloid transformation. Moreover, these findings suggest therapeutic potential for targeting the mutant forms of ASXL1 as well as miR-125 in the treatment of patients with myeloid malignancies.

Results

Mutant ASXL1 inhibited G-CSF–induced differentiation of 32Dcl3 cells. Most *ASXL1* frame-shift mutations are found in the last exon, which are predicted to result in expression of C-terminal truncated forms. We constructed an N-terminal FLAG-tagged WT ASXL1 (FLAG-ASXL1-WT) as well as N-terminal FLAG-tagged truncated mutants of ASXL1 (FLAG-ASXL1-MT1 and -MT2 (Figure 1A). FLAG-ASXL1-MT1 and -MT2 were derived from the mutated genes of 1934dupG;G646WfsX12 and 1900–1922del;E635RfsX15, respectively, of patients with MDS. Although there is some controversy as to whether the most common *ASXL1* mutation, 1934dupG;G646WfsX12, represents a true somatic mutation or an artifact (16), most studies have suggested this allele can occur as a somatic mutation in hematologic malignancies (17–19). When transiently expressed in 293T cells or stably expressed in 32Dcl3 cells, these constructs expressed ASXL1-WT and ASXL1 mutant protein (ASXL1-MT) with expected molecular weights detected by an anti-FLAG antibody (Figure 1B). As reported previously (11), immunoprecipitation studies demonstrated that EZH2 bound ASXL1-WT. We further demonstrated that ASXL1-MT as well as ASXL1-WT can bind to EZH2 (Figure 1C). ASXL1-WT could also be detected in hemopoietic cell lines by anti–C-terminal ASXL1 antibodies (Figure 1D); HL60, U937, and SET2 harboring only the ASXL1-WT alleles expressed the WT 190-kDa protein. In K562, KU812, and Mono-Mac-6 harboring 1 WT and 1 truncated mutant, ASXL1-WT could be easily detected with the C-terminal antibody. To detect C-terminal truncated endogenous ASXL1 proteins, we used antibodies against the N-terminal part of ASXL1. However, the backgrounds were so high that we could not determine whether the C-terminal–truncated ASXL1 was expressed. Similarly, in TS9;22, KBM-5, and MEG-01 cell lines harboring homozygous truncated ASXL1, we were not able to determine whether the truncated ASXL1 was expressed. We confirmed by quantitative real-time PCR (qRT-PCR) that the ASXL1 transcript was detected in these cell lines (Supplemental Figure 1; supplemental material available online with this article; doi:10.1172/JCI70739DS1). When ASXL1-MTs were expressed in 293T cells, they localized to the nucleus (Figure 1E) similar to the ASXL1-WT, suggesting that the truncated ASXL1 mutant is expressed and prompting us to examine the effects of stable expression of ASXL1-MTs in both in vitro and in vivo experiments.

We investigated the effects of expression of WT and mutant ASXL1 alleles on hematopoietic differentiation. To this end, we expressed ASXL1-MT1 and -MT2 in 32Dcl3 cells and examined their effect on differentiation of the transduced cells. Interestingly, G-CSF–induced differentiation of 32Dcl3 cells was partially inhibited by the expression of ASXL1-MT1 and -MT2 but not by the expression of ASXL1-WT, based on morphology and flow cytometric expression of CD11b (Figure 1F). In addition, all-trans retinoic acid–induced (ATRA-induced) granulocytic differentiation of HL60 and GM-CSF–induced monocytic differentiation of FDC-P1 cells were attenuated by the overexpression of ASXL1-MT2 (Supplemental Figure 2A). The expression of ASXL1-MTs as well as ASXL1-WT did not affect the growth rate of 32D cells cultured in the presence of IL-3 and did not induce factor-independent growth (Supplemental Figure 2B). For further experiments, we mainly used ASXL1-MT2 unless otherwise specified, and refer to this mutant hereafter as ASXL1-MT.

ASXL1-MT reduced the expression of Clec5a/Mdl1. To elucidate the molecular mechanisms by which ASXL1-MT inhibited the G-CSF–induced differentiation of 32Dcl3 cells, we compared the expression profiles of parental 32Dcl3 cells and 32Dcl3 cells expressing ASXL1-MT maintained in the presence of 1 ng/ml IL-3 or 50 ng/ml G-CSF. We identified a small set of genes whose expression levels changed more than 2-fold. These included *Clec5a/Mdl1*, *Cd14*, and *Prom1*. Expression of these genes was downregulated in 32Dcl3 cells expressing the ASXL1-MT. Among them, we focused on the type II transmembrane receptor Clec5a (20), because it was known that Clec5a expression is associated with granulocytic differentiation of 32Dcl3 cells (21). We confirmed that expression of *Clec5a* was reduced in 32Dcl3-expressing ASXL1-MT (Figure 2A). Moreover, while the expression of Clec5a in 32D cells was increased by G-CSF stimulation in a time-dependent manner, as previously reported (21), both in mRNA and protein levels, this increase was profoundly suppressed by the expression of ASXL1-MT but not by ASXL1-WT (Figure 2, A and B). This may result from the observation that myeloid differentiation of 32Dcl3 cells was inhibited by ASXL1-MT, and expression of Clec5a increases with myeloid differentiation, suggesting Clec5a serves as a marker of myeloid differentiation. On the other hand, ATRA or G-CSF–induced granulocytic differentiation of HL60 cells or 32Dcl3 cells, respectively, was enhanced by the expression of Clec5a (Figure 2C and